ACS APPLIED NANO MATERIALS

www.acsanm.org Review

Extended Metal–Organic Frameworks on Diverse Supports as Electrode Nanomaterials for Electrochemical Energy Storage

Kaiqiang Zhang, Kent O. Kirlikovali, Quyet Van Le, Zhong Jin, Rajender S. Varma,* Ho Won Jang,* Omar K. Farha,* and Mohammadreza Shokouhimehr*

Cite This: *ACS Appl. Nano Mater.* 2020, 3, 3964–3990 Read Online

ACCESS | Metrics & More | Article Recommendations

ABSTRACT: The incorporation of renewable and sustainable energy sources in electric grids has been acknowledged as a potential strategy to solve the ever-growing environmental issues that result from the use of fossil fuels. In order to realize the full potential of these systems, advanced electrochemical energy storage devices must be developed. Recently, researchers have turned their attention toward obtaining high-performance electrode nanomaterials in order to develop these next-generation electrochemical systems. Metal–organic frameworks (MOFs), well-known for their relatively straightforward fabrication methods, high nanoscale porosities, robust nanostructures, and intrinsic crystallinities, have emerged as a class of nanomaterials potentially capable of meeting the stringent demands for these systems. Specifically, bridged MOFs and other MOF derivatives have recently been established as the primary MOF-based nanomaterials in studies on electrochemical systems, such as batteries and capacitors, as these nanomaterials have demonstrated the potential to address the poor conductivities that arise from separated nanoparticles in early reports on MOF-only systems. As such, we have focused this review on these nanomaterials, and in particular, we discuss the advantages and disadvantages of electrochemical systems with a range of support materials, including carbon nanotubes, carbon fibers, graphene, metals, metal oxides, and conductive polymers. Finally, we highlight the remaining challenges and the possible opportunities for research in this field in order to facilitate future studies.

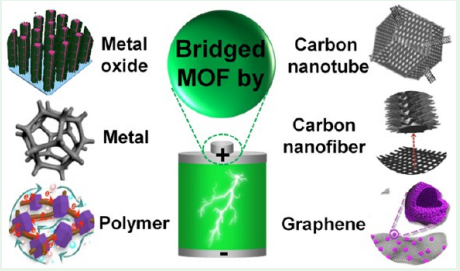

KEYWORDS: *metal–organic framework, bridging and connecting, high-performance conductivity, electrochemical energy storage, nanomaterial*

1. INTRODUCTION

Given the contradiction that is associated with the desire to reduce the use of fossil fuels due to environmental pollution despite a constant increase in society's energy demand, the implementation of green and sustainable energy resources has been pursued as an alternative energy generation strategy.[1−3] While significant advancements regarding these promising energy sources have occurred in recent years, numerous challenges still must be addressed, such as the intermittence and instability of green energy sources (i.e., solar energy and wind energy), low conversion efficiencies, and technological limitations. One of the most promising energy storage systems involves using electric energy that is stored in rechargeable batteries, which can then be utilized for various electronic devices ranging from mobile phones to laptop computers. To date, a wide variety of batteries have been developed, including metal-ion batteries, metal-air batteries, fuel cells, and solar cells.[4−6] Secondary metal-ion batteries, which use alkali metal or alkali earth metal ions as charge carriers that enable recharging of the batteries, exhibit improved energy densities due to the large capacity values and discharge potentials. To further enhance the corresponding power densities (the product of capacity and potential during unit time, W kg^{-1}) of these battery nanomaterials, different techniques have been employed for combining batteries with supercapacitors to achieve both higher energy densities (the product of capacity and potential, W h kg^{-1}) and enhanced power densities.[7,8] In the hybrid devices, battery-type anodes and capacitor-type cathodes are used to completely exploit the advantages of electrochemically active anode nanomaterials with Faradaic pseudocapacitive cathodes to yield a device with excellent energy and power densities. Therefore, the improvement in device performance primarily relies on the design and fabrication of advanced electrode nanomaterials.

Metal organic frameworks (MOFs), functional and highly porous nanomaterials constructed from metal-based nodes and organic linkers, have garnered immense attention in the context of both electrodes and electrolyte materials, and numerous MOFs with excellent electrochemical properties

Received: March 12, 2020
Accepted: April 13, 2020
Published: April 13, 2020

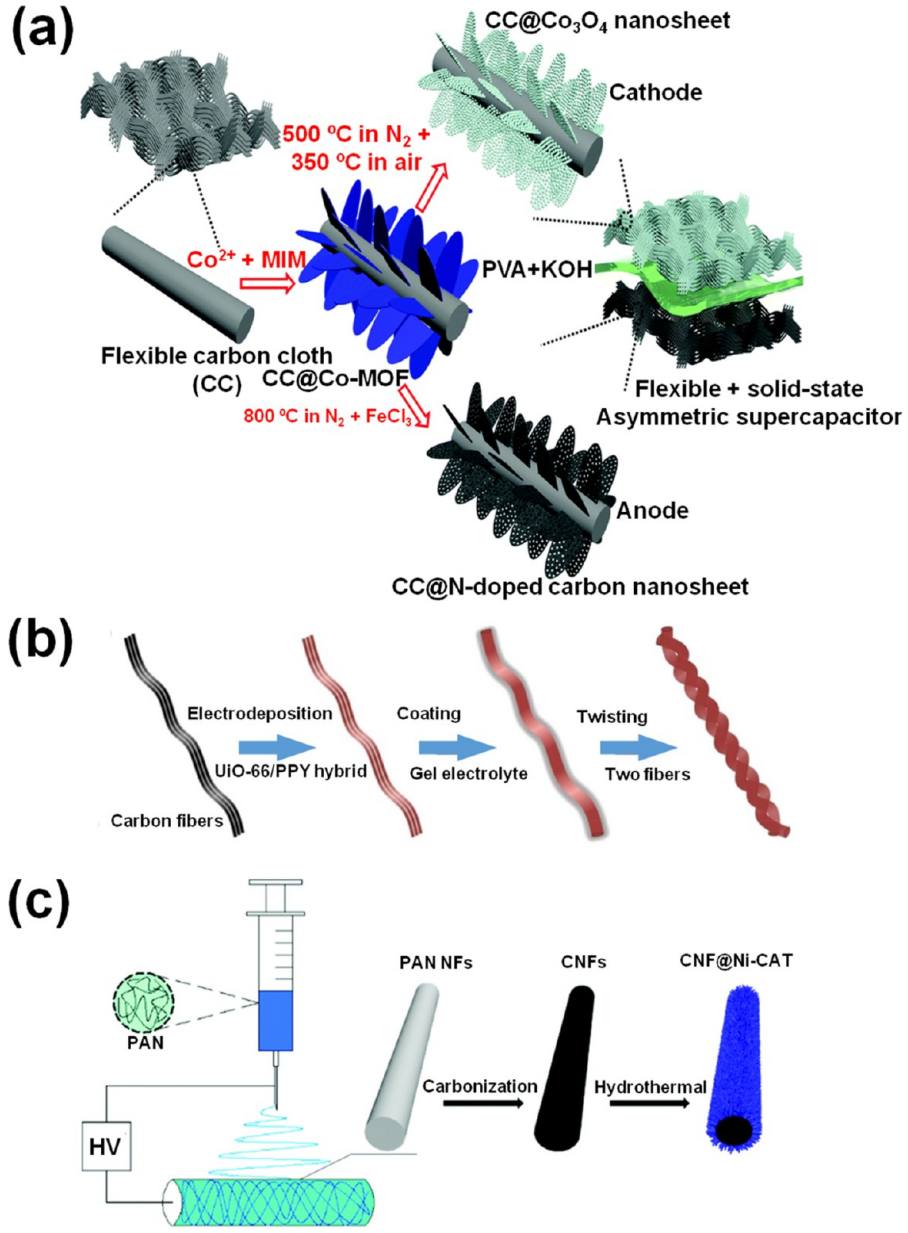

Figure 1. (a) Schematic illustration of the "one for two" fabrication process: 2D Co_3O_4 nanosheets cathode and N-doped carbon nanosheets anode are obtained from the same Co-MOF precursor and assembled into a flexible asymmetric supercapacitor. Reproduced with permission from ref 51. Copyright 2017 Royal Society of Chemistry. (b) Illustration of the fabrication of UiO-66/polypyrrole-based flexible nanofiber supercapacitor device. Reproduced with permission from ref 52. Copyright 2018 American Chemical Society. (c) Schematic illustration of the synthesis of CNF@Ni-catecholate. Reproduced with permission from ref 53. Copyright 2019 Royal Society of Chemistry.

have been documented for use in multiple types of battery systems.[9−15] The intrinsically nanoporous and crystalline frameworks are able to facilitate charge insertion, and the multiple valence states of the metal cation nodes enable electron absorption and desorption during electrochemical reactions. Furthermore, the size of the organic linkers between any two metal cation nodes generally determines the nanopore apertures, which significantly influences the charge permeability throughout the framework. Thus, these inherent properties render MOFs a promising class of nanomaterials with great potential when used in electrochemical systems.

Despite these favorable properties, some remaining issues must be addressed in order for MOFs to be employed in advanced electrochemical systems. For example, the electrostatic bonding interaction between the anionic organic linkers and cationic metal nodes results in a decrease in performance due to the consumption of charge carriers. Moreover, the majority of the MOF-based nanomaterials are electronic insulators, which is a serious disadvantage in the context of electrode materials, as poor conductivity results in electrode polarization and suppressed electrochemical dynamics, ultimately leading to reduced efficiencies of electrochemically active nanomaterials. In order for MOF-based electrode nanomaterials to be employed in high-performance electrochemical systems, researchers must improve the inherently low conductivities of these nanomaterials.

In particular, the introduction of "bridging" support materials, such as carbon fibers or graphene,[16−25] has emerged as a promising method to address the poor electronic conductivity and the agglomeration of the native MOF

https://dx.doi.org/10.1021/acsanm.0c00702
ACS Appl. Nano Mater. 2020, 3, 3964−3990

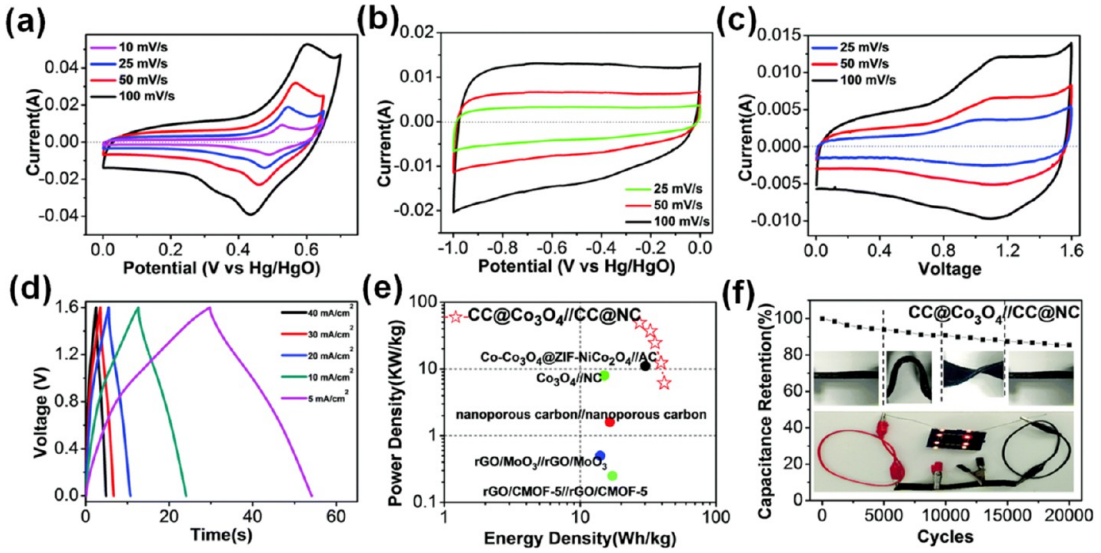

Figure 2. Electrochemical performances: (a−c) CV curves, (d) charge−discharge curves, (e) Ragone plots, and (f) the cycling test result of the asymmetric supercapacitor with Polyvinyl Acetate-KOH gel electrolyte. Reproduced with permission from ref 51. Copyright 2017 Royal Society of Chemistry.

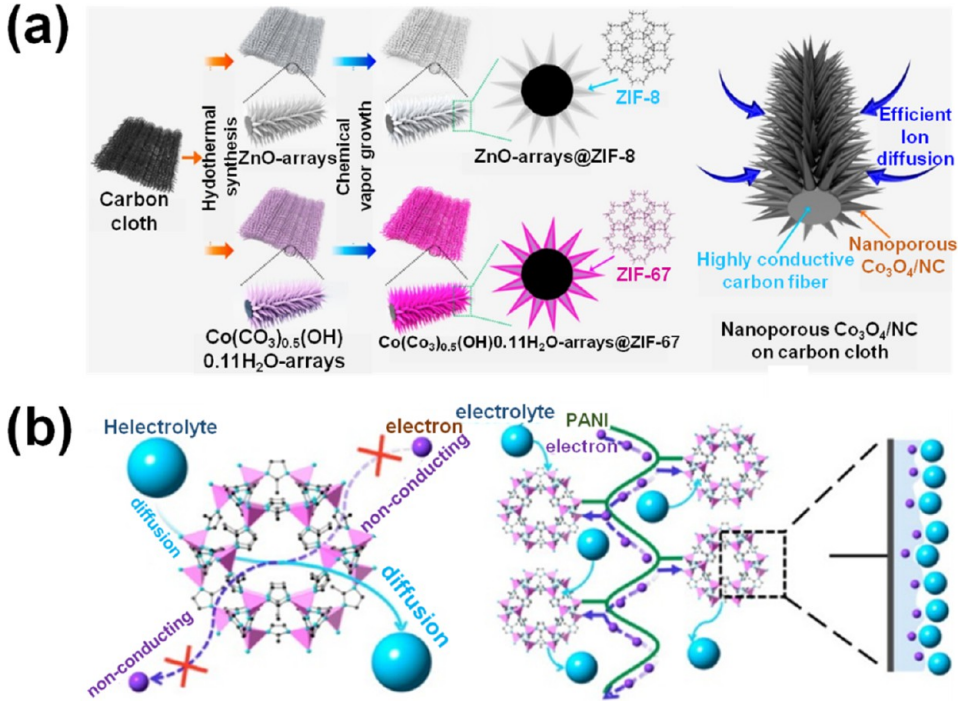

Figure 3. (a) Schematic illustration for the synthesis process of different electrode nanomaterials. Reproduced with permission from ref 54. Copyright 2018 American Chemical Society. (b) Schematic representation of electron and electrolyte conduction in a MOF and a MOF interwoven by polyaniline. Reproduced with permission from ref 58. Copyright 2015 American Chemical Society.

nanomaterials; therefore, this implies that the material design plays a significant role in the improvement of these systems.[26−32] Although numerous reports on this topic have focused on composite MOF-based electrode nanomaterials, few reports have emphasized the bridging effect when discussing connecting MOFs or MOF-derived nanomaterials.[33−45] Therefore, we have reviewed reports on bridged MOFs and MOF-derived electrode nanomaterials for use in electrochemical applications, such as batteries and capacitors, with a focus on the material designs that yield sufficient structural integrity as well as high electronic and ionic conductivities. We have organized the discussion based on the type of bridging materials used, which include carbon nanofibers (CNFs), carbon nanotubes (CNTs), graphene, metals, metal oxides, and conductive polymers. Additionally, we have highlighted material design principles regarding this class of materials and summarized the advantages and disadvantages of each type of bridging material. Finally, we discuss remaining challenges and the corresponding opportunities for researchers in this community, with the hopes of stimulating future studies.

https://dx.doi.org/10.1021/acsanm.0c00702
ACS Appl. Nano Mater. 2020, 3, 3964−3990

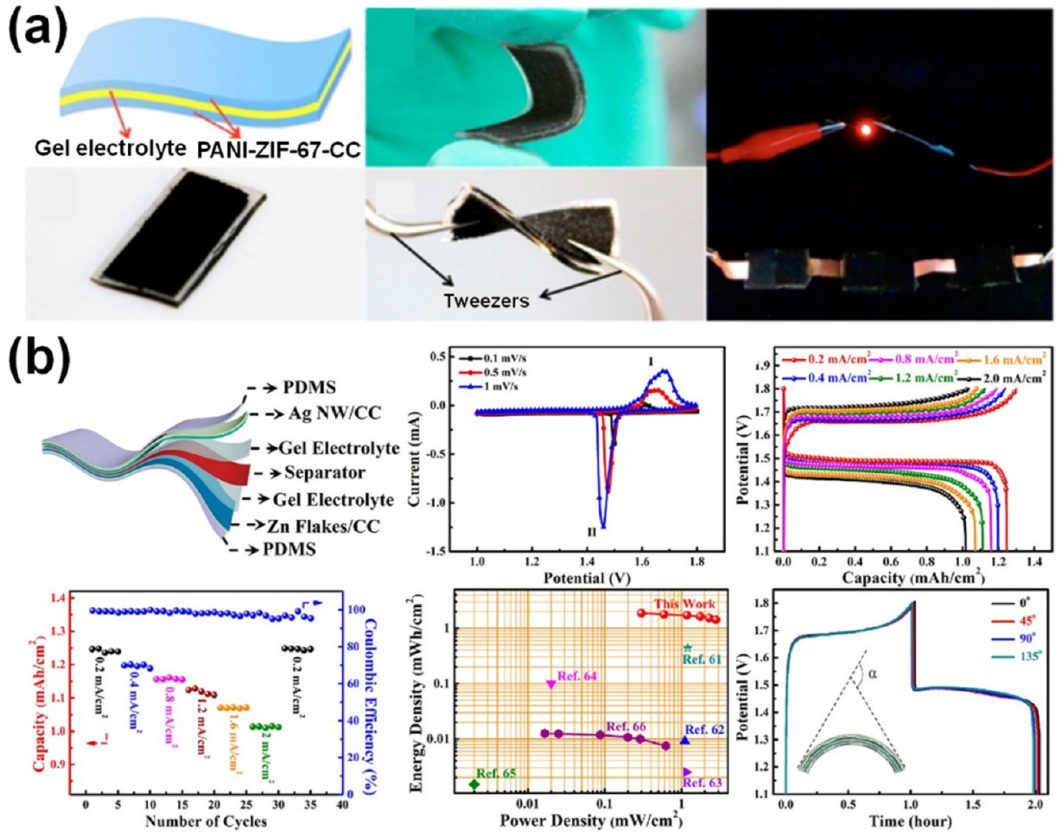

Figure 4. (a) Schematic illustration of polyaniline−ZIF-67−carbon cloth flexible solid-state SC device. Reproduced with permission from ref 58. Copyright 2015 American Chemical Society. (b) Schematic diagram and performances of the fabricated flexible quasi-solid-state Ag−Zn battery: CV curves at different scan rates, galvanostatic charge/discharge curves, rate performances, Ragone plots, and galvanostatic charge/discharge curves of a device bent at various angles. Reproduced with permission from ref 62. Copyright 2018 American Chemical Society.

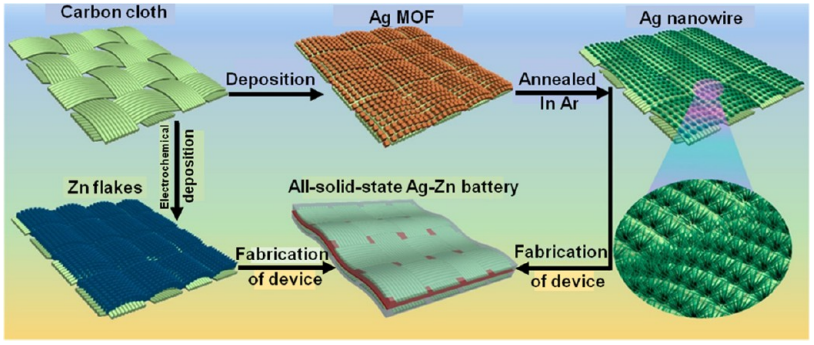

Figure 5. Schematic illustration of the synthesis of the flexible quasi-solid-state Ag−Zn battery. Reproduced with permission from ref 62. Copyright 2018 American Chemical Society.

2. SUPPORTED MOFS

2.1. Carbon Nanofiber (CNF). *2.1.1. Natural CNF.* CNF is a promising current collector due to its high electronic conductivity and inherent flexibility, and numerous CNF-supported electrode nanomaterials have been reported with superior electrochemical performances in devices relative to the non-CNF analogues.[46−48] Typically, carbon fiber supported electrode nanomaterials are synthesized in a high-temperature and high-pressure environment in which the desired nanomaterials are grown on the carbon fiber surfaces, with solvothermal and hydrothermal methods among the most common. This synthetic strategy enables the growth of the active nanomaterials with various morphologies, and the highly conductive CNF supports provide smooth electronic flow channels that ensure an adequate supply of electrons during electrochemical reactions. Furthermore, the supported material structure can effectively widen the contact surface area between the active materials and the electrolyte to attain a high-use ratio of active material in the sample. The inherent flexibility of CNFs imparts a significant mechanical tolerance to the active materials for fabricating multishaped devices. In this section, we have summarized CNF-supported MOFs or MOF derivatives for use in electrochemical applications.

The use of CNF-interwoven carbon cloth as a support material in bridging MOFs or MOF derivatives results in significant improvements in conductivity. For example, Liu and co-workers designed carbonized MOF arrays supported by CNFs and employed them for use in supercapacitors.[49]

https://dx.doi.org/10.1021/acsanm.0c00702
ACS Appl. Nano Mater. 2020, 3, 3964−3990

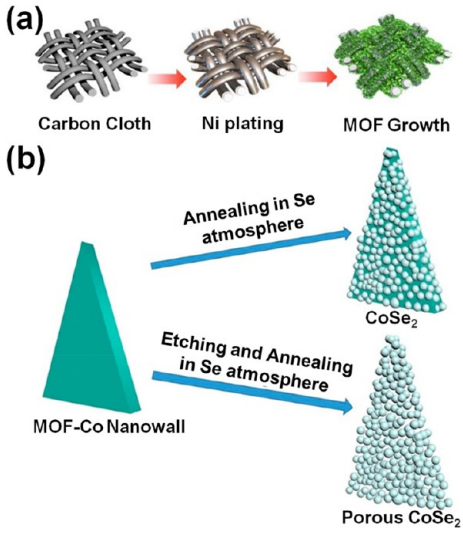

Figure 6. (a) Schematic illustration of the preparation of a NiCo-MOF cathode. Reproduced with permission from ref 64. Copyright 2019 Elsevier. (b) Schematic illustration of the formation for porous $CoSe_2$ and $CoSe_2$. Reproduced with permission from ref 65. Copyright 2017 American Chemical Society.

Through careful control experiments, it was found that the supercapacitor contributes an energy density of 124.8 μW h cm^{-2} under the power density of 2.55 mW cm^{-2}. More importantly, the use of CNFs renders the supercapacitor flexible, even when it is used with hard carbon-based electrode materials.

The incorporated flexibility by using CNFs as active material supports has been further demonstrated by Li and co-workers.[50] In this study, the authors fabricated CNF-supported MOFs with a cactus-like morphology via a hydrothermal method. The optimized composite electrode exhibits a high specific capacitance of approximately 1100 F g^{-1}, and the assembled full-cell displays an energy density of approximately 34 W h kg^{-1} based on the specific capacitance of approximately 100 F g^{-1}. The authors emphasized the flexibility obtained from the use of CNFs. In a related study, Guan and co-workers used a single MOF precursor to fabricate a porous carbon- and metal oxide-based electrode for use in the same supercapacitor, which was achieved through the etching and exposed heating of the carbonized MOFs (Figure 1a).[51] This system demonstrates robust mechanical flexibility, as the outstanding electrochemical performances and high capacitance values are retained under a variety of bending treatments. The fabricated asymmetric supercapacitors exhibit superior power and energy densities (41.5 W h kg^{-1} at a power density of 6.2 kW kg^{-1}) in comparison with the other supercapacitors (Figure 2a).

Owing to the flexible nature of CNF-based electrodes, a wearable supercapacitor has been demonstrated by Qi and co-workers in which the authors deposited the MOF/polypyrrole composite through a one-pot electrodeposition strategy (Figure 1b).[52] This strategy resulted in an all-solid-state supercapacitor with specific capacitance, power density, and

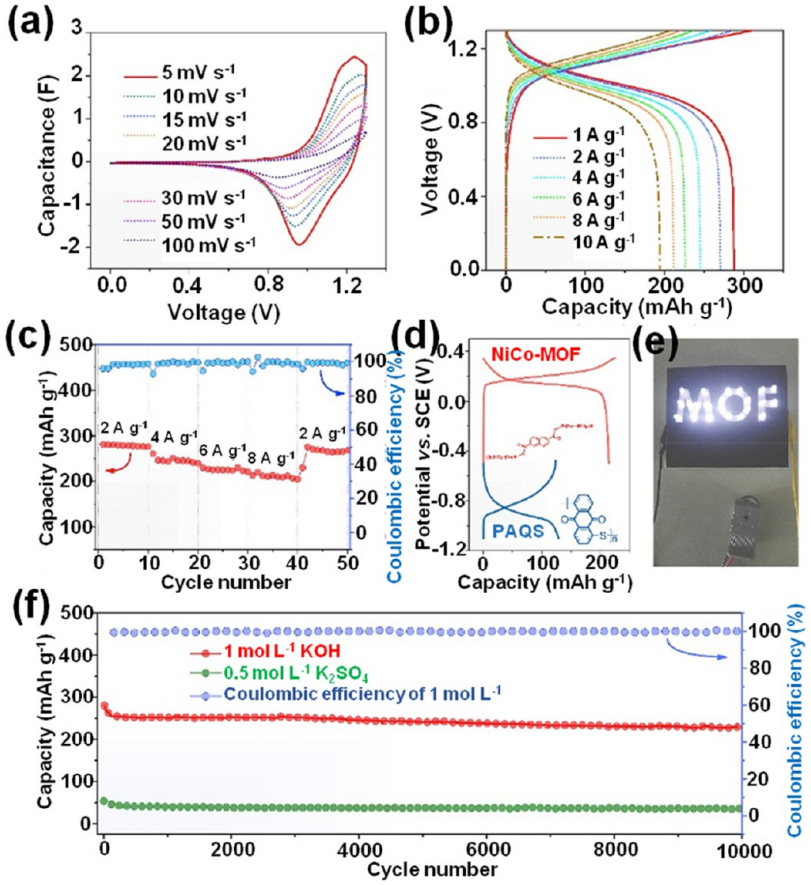

Figure 7. Electrochemical performances: (a) CV plots, (b) charge/discharge profiles, (c) rate capacity, (d) charge/discharge profiles, (e) photograph of the full cell lighting up LEDs, and (f) cycle stability. Reproduced with permission from ref 64. Copyright 2019 Elsevier.

https://dx.doi.org/10.1021/acsanm.0c00702
ACS Appl. Nano Mater. 2020, 3, 3964−3990

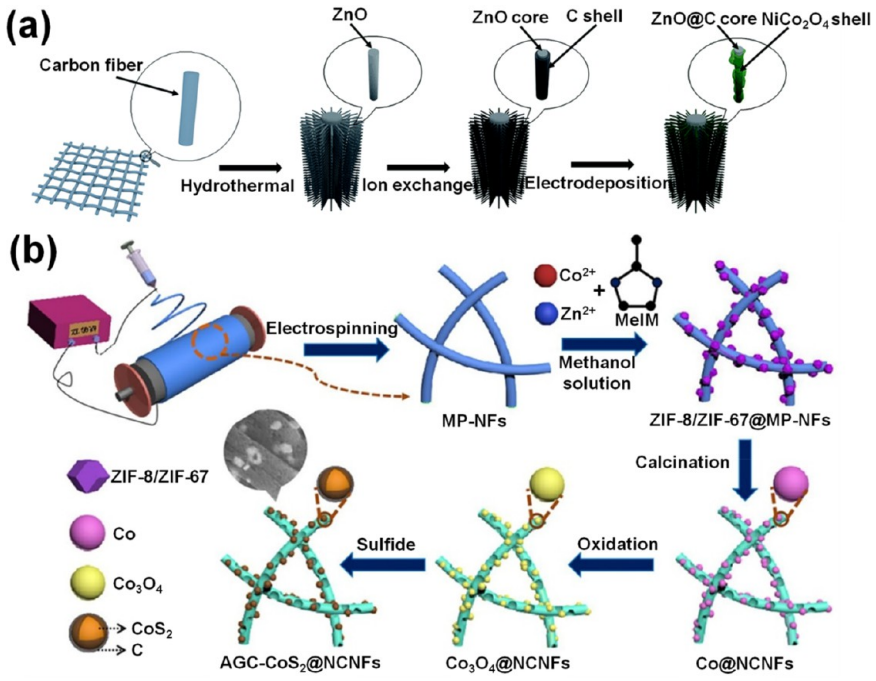

Figure 8. (a) Schematic illustration of the fabrication of ZnO@C@$NiCo_2O_4$ nanorod sheet arrays. Reproduced with permission from ref 66. Copyright 2016 Royal Society of Chemistry. (b) Schematic illustration of the synthesis of amorphous and graphite carbon−CoS_2@NCNFs. Reproduced with permission from ref 67. Copyright 2020 Elsevier.

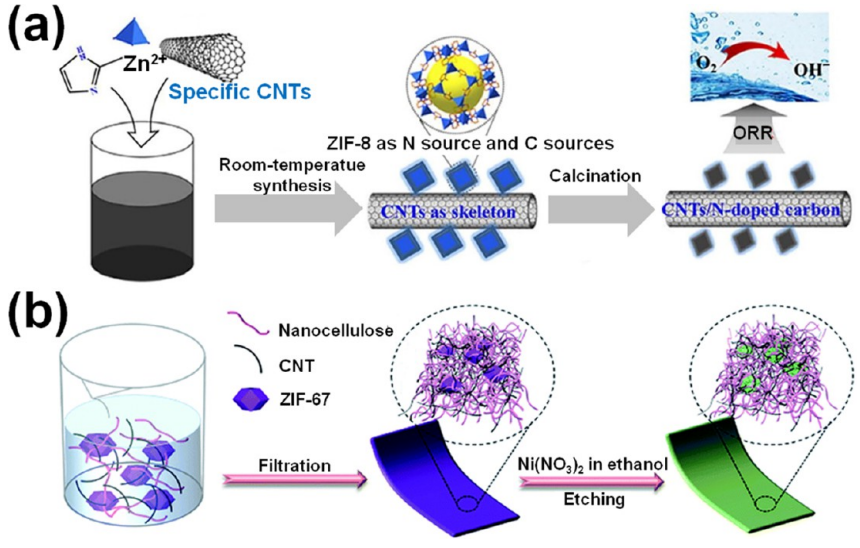

Figure 9. (a) The schematic synthesis of nitrogen-doped porous carbon materials from ZIF-8/CNTs composites. Reproduced with permission from ref 71. Copyright 2017 Science China Press. (b) Schematic illustration of the formation process of layered double-hydroxide−carbon cloth−CNT nanosheets. Reproduced with permission from ref 72. Copyright 2018 Royal Society of Chemistry.

energy density values of 206 mF cm^{-2}, 2102 μW cm^{-1}, and 12.8 μW h cm^{-1}, respectively. Strikingly, the fabricated device exhibits temperature and mechanical compatibility even under extreme environments, such as repeated bending (360°) and heating/cooling (100 to −15 °C) (Figure 1c). Zhao and co-workers reported a free-standing supercapacitor electrode by growing the MOFs on core−shell type carbon fibers that were formed by electrospinning, followed by a carbonization treatment (Figure 1c).[53] The composite electrode provides a capacitance of up to 502.95 F g^{-1} at a current density of 0.5 A g^{-1}, which was attributed to the synergetic effect between the CNFs and Ni-catecholate. Finally, good electrochemical performance with this device was obtained, with an energy density of 18.67 W h kg^{-1} under a power density of 297.12 W kg^{-1}. In this work, the use of CNFs efficiently solved the agglomeration issue of two-dimensional MOFs. Young and co-workers demonstrated that the CNF-supported ZIF-8 and ZIF-67 materials are compatible with supercapacitors.[54] The ZIF-8 and ZIF-67 frameworks were grown on rod-type metal oxide cores, followed by a heat treatment to yield conductive metal oxides encapsulated inside the nanoporous carbon framework (Figure 3a). When employed as electrode materials in supercapacitors, the Co_3O_4/nanoporous carbon hybrid elec-

https://dx.doi.org/10.1021/acsanm.0c00702
ACS Appl. Nano Mater. 2020, 3, 3964−3990

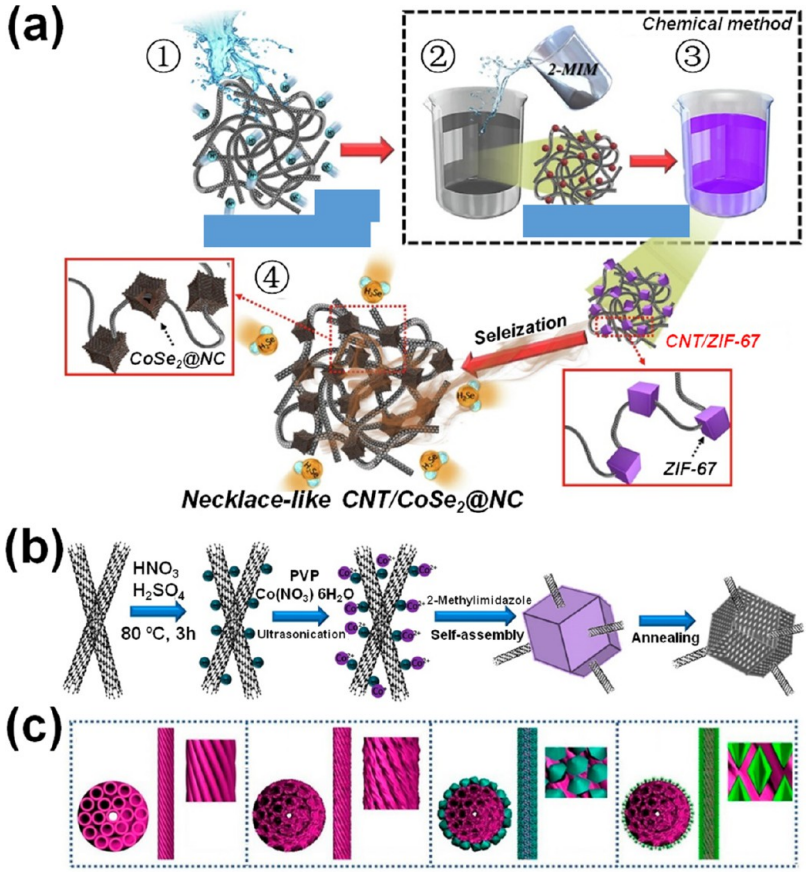

Figure 10. (a) Formation mechanism of necklace-like mesoporous CNT/$CoSe_2$@N-doped carbon composite. Reproduced with permission from ref 76. Copyright 2019 Elsevier. (b) Schematic illustration of the procedure used to fabricate multiwall CNTs/Co_3O_4. Reproduced with permission from ref 77. Copyright 2015 American Chemical Society. (c) Schematic of the synthesis process of the spindle-like-α-Fe_2O_3@C/oxidized carbon nanotube fiber electrode. Reproduced with permission from ref 78. Copyright 2018 American Chemical Society.

trode exhibited a high capacitance of 1.22 F cm^{-2} at a current density of 0.5 mA cm^{-2}.

Srimuk and co-workers introduced a facile approach for preparing electrode nanomaterials for supercapacitors in which carbon fiber paper was employed as a conductive substrate and graphene was used as a conductive agent.[55] Consequently, the synthesized carbon fiber paper-supported Hong Kong University of Science and Technology-1 MOF/reduced graphene composite exhibited a superior capacitance (385 F g^{-1} at a current density of 1 A g^{-1}). Liu and co-workers studied CNF-reinforced three-dimensional polyhedral network materials in which the highly porous features were prepared by sacrificing a MOF.[56] In this study, the CNF was fabricated by electrospinning a *N*,*N*-dimethylformamide-dissolved polyacrylonitrile solution and subsequent heat treatment. Similarly, Xu and co-workers developed an asymmetric hybrid supercapacitor by using a MOF as a precursor for fabricating mesoporous carbon nanosheets.[57] The as-fabricated mesoporous carbon nanosheets are doped with different species according to their function as a cathode or anode ($Na_3V_2(PO_4)_3$ species for cathode, VO_2 species for anode). As a result, the fabricated quasi-solid-state sodium-ion capacitors have been demonstrated to exhibit excellent electrochemical performances (78% retention after 2000 cycles at a current density of 1 A g^{-1}).

A dual-conductive layer structure has been demonstrated by Wang and co-workers in which an interconnected conductive net was formed by polyaniline and a carbon cloth located at the upper and the lower layers, respectively.[58] Between these two layers, a MOF layer is embedded; this sandwich-type composite material was used as an electrode material in a flexible solid-state supercapacitor (Figure 4a), displaying a high capacitance of up to 2146 mF cm^{-2} at 10 mV s^{-1}. Guan and coauthors synthesized CNF-supported porous metal oxide plates and studied their electrochemical performance as electrode materials for supercapacitors and in the context of electrocatalytic reactions.[59] These materials were synthesized using a wet chemical etching technique followed by heat treatment, and the resulting hollow electrode exhibited an excellent rate capability (85.6% of capacitance is retained at an 8-fold increase in the current density) and a long life-span (86.7% of the capacitance is preserved after 20000 charge/discharge cycles at a current density of 5 mA cm^{-2}). Ke and coworkers synthesized a carbon fiber-supported H-TiO_2@$Ni(OH)_2$ heterostructure using a wet chemical method, and the resulting material was employed in a high-performance supercapacitor.[60] The authors noted several key considerations for electrode materials that result in supercapacitors with excellent performance, including a large specific surface area, an improved electronic conductivity, and a high cation intercalation/deintercalation that can synergistically facilitate excellent electrochemical performances.

By hydrothermally growing bismuth-based MOFs on CNFs, Zhang and co-workers fabricated CNF-supported bismuth-doped carbon arrays, and this composite electrode nanomaterial was observed to demonstrate outstanding properties in

https://dx.doi.org/10.1021/acsanm.0c00702
ACS Appl. Nano Mater. 2020, 3, 3964−3990

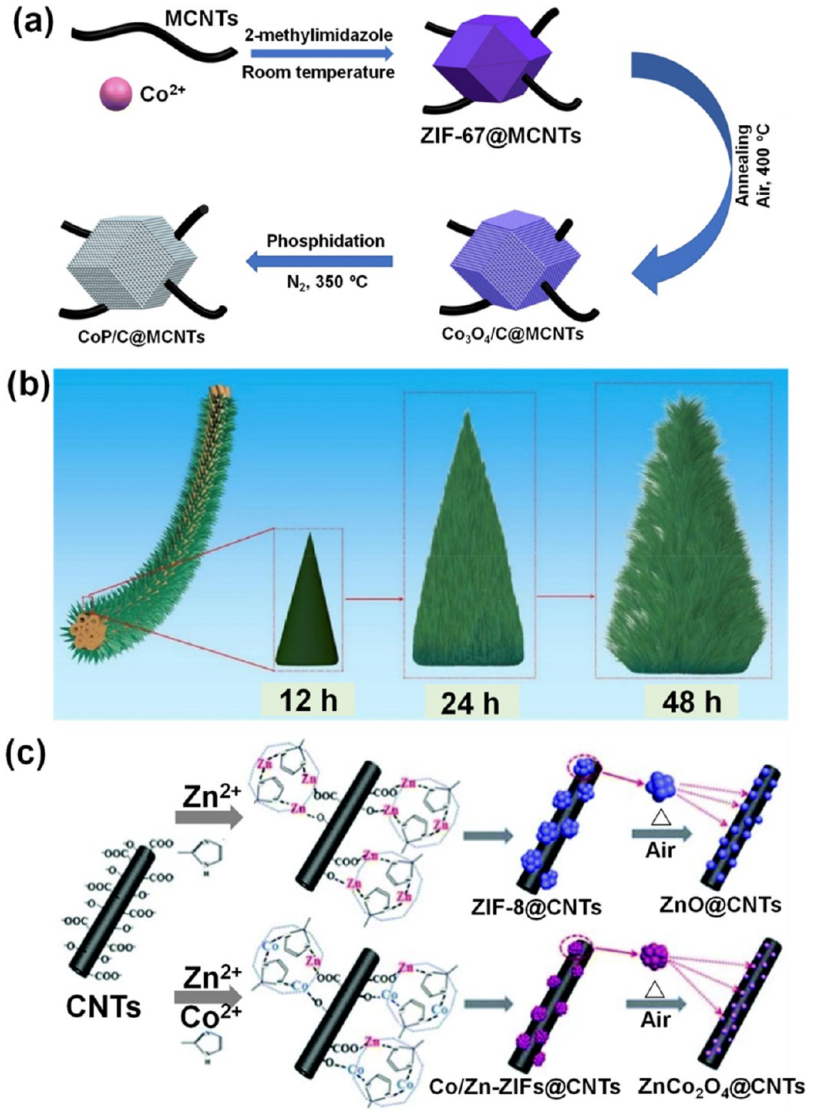

Figure 11. (a) Schematic illustration for the preparation of a CoP/C@multiwalled carbon nanotubes sample. Reproduced with permission from ref 79. Copyright 2019 Springer. (b) Schematic illustration of the preparation process for the V-MOF@carbon nanotube fiber. Reproduced with permission from ref 80. Copyright 2019 Elsevier. (c) Schematic illustration of the preparation of ZnO@CNTs and $ZnCo_2O_4$@CNTs composites. Reproduced with permission from ref 81. Copyright 2019 Royal Society of Chemistry.

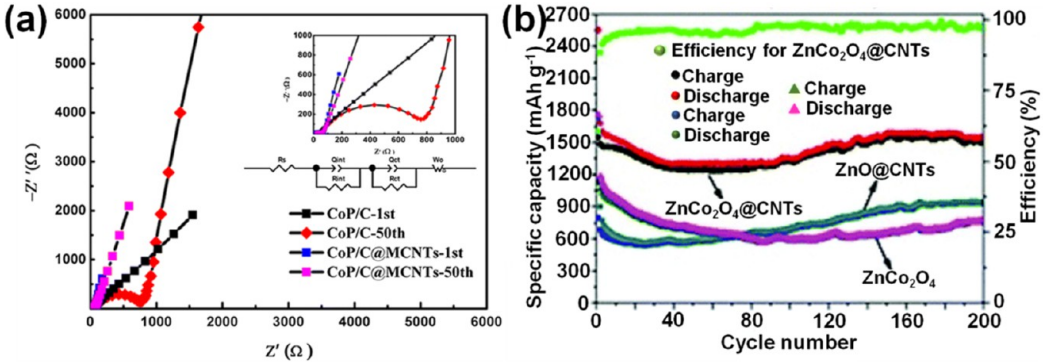

Figure 12. (a) Nyquist plots of the CoP/C@multiwalled carbon nanotubes and CoP/C electrodes before a cycle and after the 50th cycle. Reproduced with permission from ref 79. Copyright 2019 Springer. (b) Cycling performances of the $ZnCo_2O_4$@CNTs, ZnO@CNTs, and $ZnCo_2O_4$ samples at 100 mA g^{-1}. Reproduced with permission from ref 81. Copyright 2019 Royal Society of Chemistry.

the context of sodiation and desodiation.[61] The generation of many active sites and boundaries facilitates rapid sodium ion storage kinetics that are generated through the incorporation of bismuth within the highly conductive and flexible CNFs. Li and co-workers fabricated a solid-state aqueous Ag−Zn battery system by using carbon cloth that serves as a current collector

https://dx.doi.org/10.1021/acsanm.0c00702
ACS Appl. Nano Mater. 2020, 3, 3964−3990

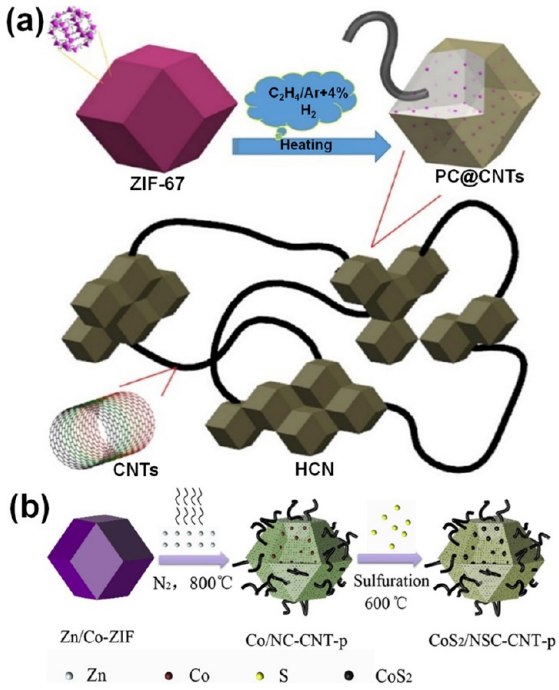

Figure 13. (a) Schematics of the synthesis of carbon nanotube hybrids. Reproduced with permission from ref 83. Copyright 2018 Elsevier. (b) Schematic of the formation process of porous N,S-*co*-doped carbon-supported CoS_2. Reproduced with permission from ref 85. Copyright 2019 Elsevier.

for both anodic and cathodic materials (Figure 5a).[62] By taking advantage of the fast electrochemical dynamics and numerous reaction sites of the MOF-derived Ag electrode (Figure 4b), the fabricated flexible battery exhibits a high capacity value of 1.87 mW h cm^{-2}. Guan and co-workers demonstrated that a hollow Co_3O_4 nanosphere encapsulated inside the porous carbon cloth-based arrays can be employed in flexible solid-state zinc−air batteries.[63] The carbon cloth provides a large degree of flexibility for these solid-state batteries, yielding excellent electrochemical performance when the device was either bent or flat, which was mainly attributed to the carbon cloth support and unique-structuring of the composite nanomaterial.

2.1.2. Derived CNFs. Electrospinning is a well-known method for the preparation of carbon nanofiber precursors, and this strategy allows for different types of species to be introduced during the synthetic process to yield functionalized carbon nanofibers. Using this technique, Zhang and co-workers demonstrated that the hierarchical $NiCo_2O_4$/NiO/CNF composite can be used as a high-performance electrode material for sodium-ion storage, exhibiting a sodium-ion storage capacity of 210 mA h g^{-1} at a specific current of 100 mA g^{-1}. A simultaneous improvement in both electronic and ionic conductivities can be simultaneously achieved by using carbon nanofibers as supports as well as by employing an expended atomic interplanar spacing of active materials. Li and co-workers designed innovative MOF materials with an expended interspace produced by organic pillars (Figure 6a),[64] and by using the materials with high electronic and ionic conductivities, the fabricated alkaline batteries exhibit a high capacity retention of 82% when the current densities increase from 1 to 20 A g^{-1}. Furthermore, the assembled cell containing a cathode comprised of the expended MOF and an organic anode exhibited a high capacity of 280 mA h g^{-1} and a long lifespan (Figure 7). A similar concept has been demonstrated by Chen and co-workers, in which the authors improved both the electronic and ionic conductivities of a MOF-based nanomaterial by using a combination of CNFs and a highly porous $CoSe_2$ that was prepared by etching the MOF template, followed by an annealing treatment (Figure 6b).[65] Consequently, this material exhibits excellent performance in a variety of supercapacitor-based applications (713.9 F g^{-1} at a current density of 1 mA cm^{-2} and 92.4% capacitance retention after 5000× cycles at 5 mA cm^{-2}) as well as in the oxygen evolution reaction (1.48 V vs H^+/H_2 onset potential). Zeng and co-workers fabricated $NiCo_2O_4$ nanosheets arrayed on the carbon fiber-supported ZnO@C nanorods and studied the electrochemical performance of this composite material when used as an electrode material for supercapacitors (Figure 8a).[66] This electrode exhibited an excellent electrochemical performance with an areal capacitance of 3.18 F cm^{-2} at a current density of 6 mA cm^{-2} and 2650 F g^{-1} at a specific current of 5 A g^{-1}. Furthermore, a sufficient capacitance of 1.21 F g^{-1} was demonstrated at a significantly higher current density of 36 mA cm^{-2}, and a reasonable cycling stability was demonstrated, as 76% of the capacitance is retained after 4000 charge/discharge cycles at a current density of 10 mA cm^{-2}. Zhang and co-workers employed a modified electrospinning strategy to fabricate CoS_2 on highly porous carbon fiber supports for use as an anode material in sodium-ion batteries.[67] Specifically, the fabrication process was conducted via a three-step heat treatment process: carbonization, oxidation, and sulfuration (Figure 8b), and the prepared electrode exhibited a superior

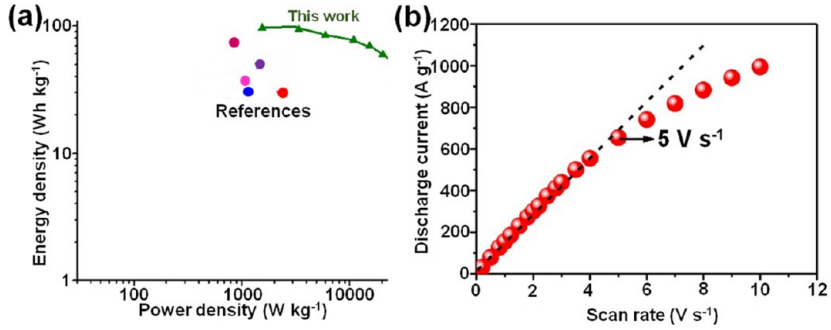

Figure 14. (a) Ragone plot of the assembled symmetric supercapacitor device compared with reported mixed MOFs-based supercapacitor devices. Reproduced with permission from ref 103. Copyright 2019 Elsevier. (b) Discharging current vs scan rate with a linear dependence up to 5 V s^{-1}. Reproduced with permission from ref 111. Copyright 2016 Elsevier.

https://dx.doi.org/10.1021/acsanm.0c00702
ACS Appl. Nano Mater. 2020, 3, 3964−3990

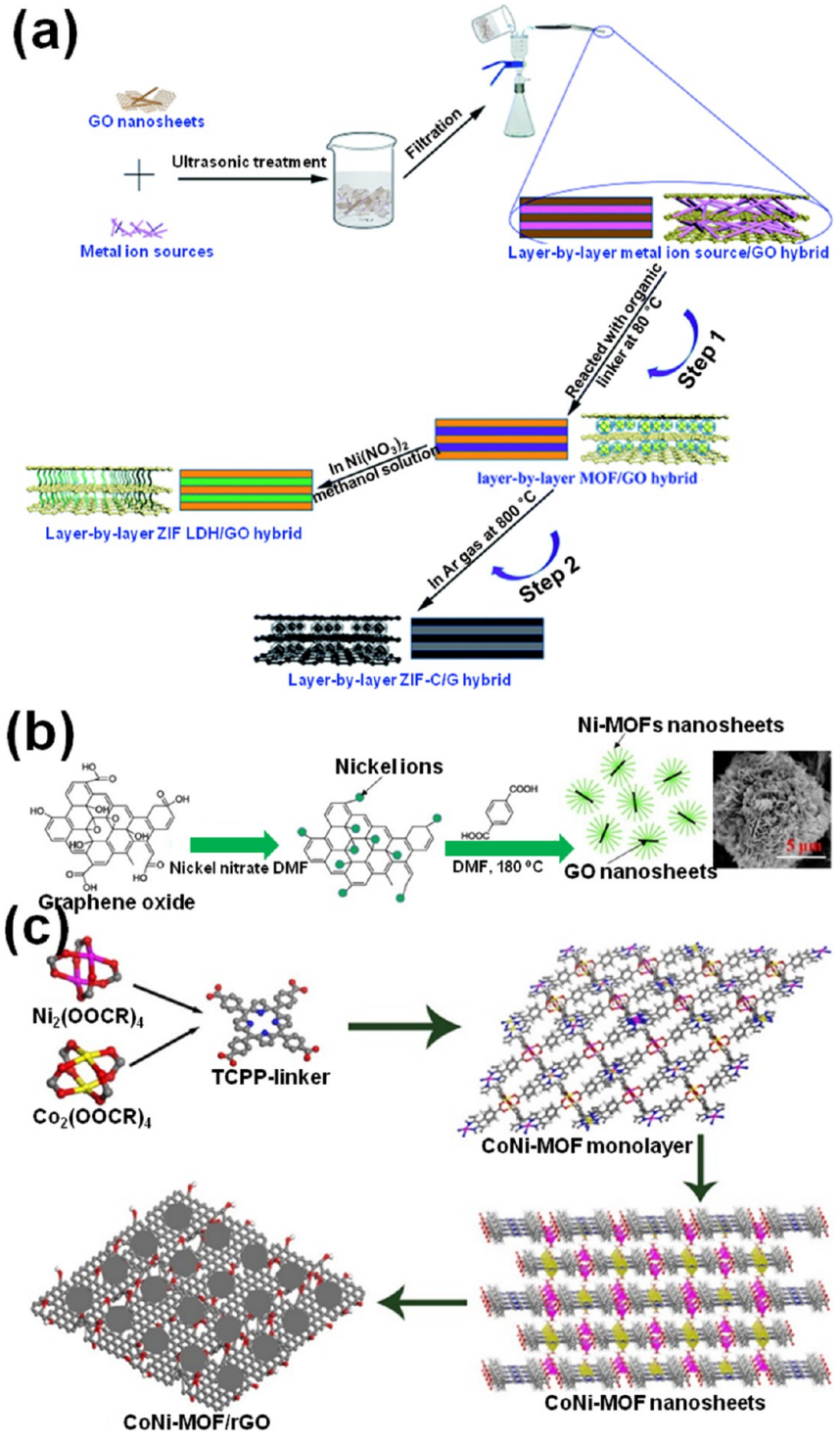

Figure 15. (a) Schematic representation of the synthesis route to layer-by-layer MOF/GO hybrid films. Reproduced with permission from ref 108. Copyright 2017 Royal Society of Chemistry. (b) Illustration of an *in situ* hybrid of Ni-MOFs with graphene oxide nanosheets. Reproduced with permission from ref 109. Copyright 2016 American Chemical Society. (c) Schematic illustration of the preparation of the CoNiMOF/rGO catalyst. Reproduced with permission from ref 110. Copyright 2019 American Chemical Society.

electrochemical performance in terms of the capacity (876 mA h g^{-1} at 100 mA g^{-1}) and cycling stability (148 mA h g^{-1} at 3.2 A g^{-1}). Ren and co-workers elucidated the conductivity and structural integrity enabled by carbon fibers by preparing MoS_2 nanosheets@N-doped carbon nanowall arrays that were composed of MOFs and studied the electrochemical performance of this composite material as an anode in sodium-ion batteries.[68] The fabricated electrode exhibited excellent properties of 619.2 mA h g^{-1} (200 mA g^{-1}) and 265 mA h g^{-1} after 1000 cycles (1 A g^{-1}).

Overall, CNFs comprise a promising, low-cost class of support or bridging materials employed for composite electrodes that are potentially suitable for practical applications. These materials exhibit good electronic conductivities, providing a sufficient supply of electrons during the electrochemical reactions at high current densities. Furthermore, the

https://dx.doi.org/10.1021/acsanm.0c00702
ACS Appl. Nano Mater. 2020, 3, 3964−3990

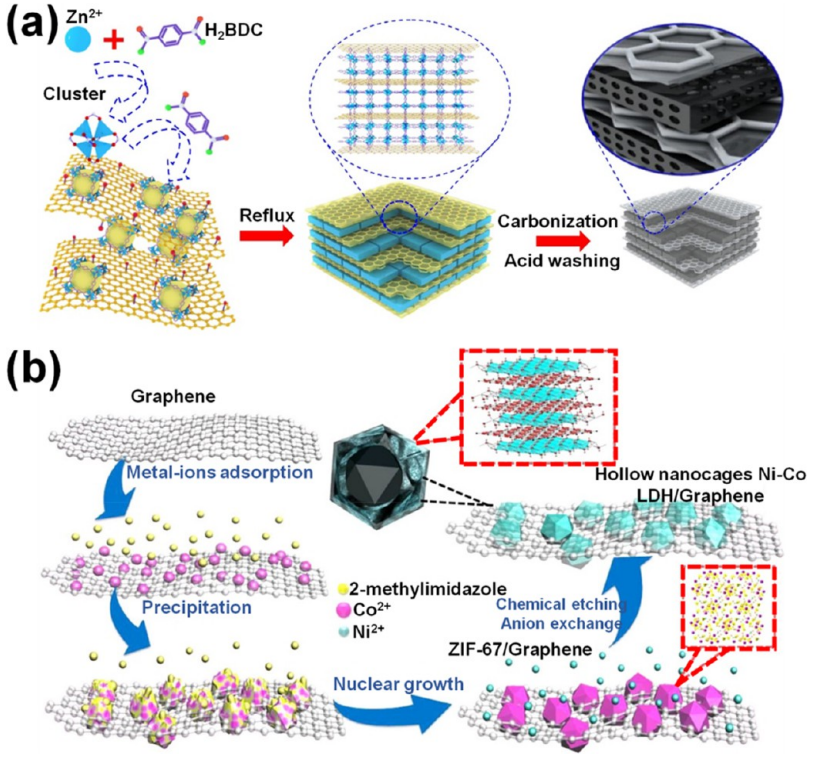

Figure 16. (a) Schematic illustration showing the fabrication process for porous carbon building using MOFs and graphene oxide as precursors. Reproduced with permission from ref 111. Copyright 2016 Elsevier. (b) Schematic illustration of the synthesis procedure of the Ni−Co layered double hydroxide hollow nanocages/graphene composite. Reproduced with permission from ref 112. Copyright 2017 American Chemical Society.

high mechanical strength, combined with the flexible fiber shape, enables the formation of foldable electrodes for use in wearable devices. On the other hand, a specific manufacturing process is required for growing the MOFs or MOF derivatives on the CNFs, which may increase the complexity of the manufacturing process.

2.2. Carbon Nanotubes (CNTs). CNTs, including single-wall CNTs and multiwall CNTs, are robust support materials with appropriate electronic conductivities for use in electrochemical systems. CNTs, which have hollow structural features, differ from the densely packed internal structures of CNFs; the larger degree of porosity in CNTs may allow for better mass transfer properties relative to those of CNFs. In addition, similar to carbon nanofibers, carbon nanotubes exhibit mechanical flexibility and high conductivity, and the nanotube-based systems are perhaps even more advantageous than their nanofiber counterparts, as better electrolyte infiltration and lower weights have been observed in CNT-based materials, resulting in better rate performances and greater energy densities. Given the numerous reports on the CNT-supported MOFs and MOF derivatives,[69,70] we focused on two prevalent and main systems in this section: (1) rooted CNT supports and (2) *in situ* grown CNT supports.

2.2.1. Rooted CNT Supports. Rooted CNTs, also known as introduced CNTs, are classified as a type of CNT-containing material prepared by the introduction of CNTs inside the product. While this strategy can effectively improve the conductivity, generating uniform dispersions of CNTs inside the product has not proven straightforward in some cases. Tan and co-workers prepared a MOF-derived, CNT-connected porous carbon nanomaterial (Figure 9a) that demonstrated high-performance both when employed in a supercapacitor (75.1 F g^{-1} at a current density of 1 A g^{-1}) and when used in the oxygen reduction reaction (the reduction current density is comparable to that of the noble metal-containing Pd/C catalyst).[71] The authors attributed the superior performance to the combination of suitable conductivity (~5 Ω in charge transfer), favorable porosity (1249.1 m^2 g^{-1}, 0.53 cm^3 g^{-1}), and accessible nitrogen dopant species benefiting from the hierarchical porosity. Xu and co-workers fabricated a flexible and foldable electronic device composed of CNTs and a nanocellulose-supported zeolitic imidazolate framework-67 (Figure 9b).[72] A solid-state device fabricated by the electrode and PVA/KOH gel electrolyte exhibited an areal capacitance of 168 mF cm^{-2} and an energy density of 0.6 mW h cm^{-3} at a power density of 8.0 mW cm^{-3}, which is much lower than that in the half-cell (1979 mF cm^{-2}), suggesting that researchers should consider properly matching the anode and cathode. The well matching factor of an anode and a cathode is also emphasized by previous reports in which the authors not only demonstrated new electrode materials but also studied the matching between anodes and cathodes.[73−75] After employing ZIF-67 growing on CNTs as a precursor, Yang and co-workers performed a selenization reaction to synthesize $CoSe_2$@C nanoparticles connected by CNTs (Figure 10a).[76] This material exhibited excellent sodium-ion storage with high specific capacity values and good rate capabilities (404 mA h g^{-1} at a current density of 0.2 A g^{-1} and 363 mA h g^{-1} at a current density of 5.0 A g^{-1}), which was attributed to the favorable interaction between the $CoSe_2$@C active nanomaterial and the CNT host. In addition to building on CNT supports to yield a CNT@product texture, CNTs can also be used to form a skewered, rod-like structure with MOFs or MOF derivatives during the synthesis. For example, Huang and co-workers grew MOF precursors on the CNT hosts followed by a heat treatment process to generate a multiwall CNT/

https://dx.doi.org/10.1021/acsanm.0c00702
ACS Appl. Nano Mater. 2020, 3, 3964−3990

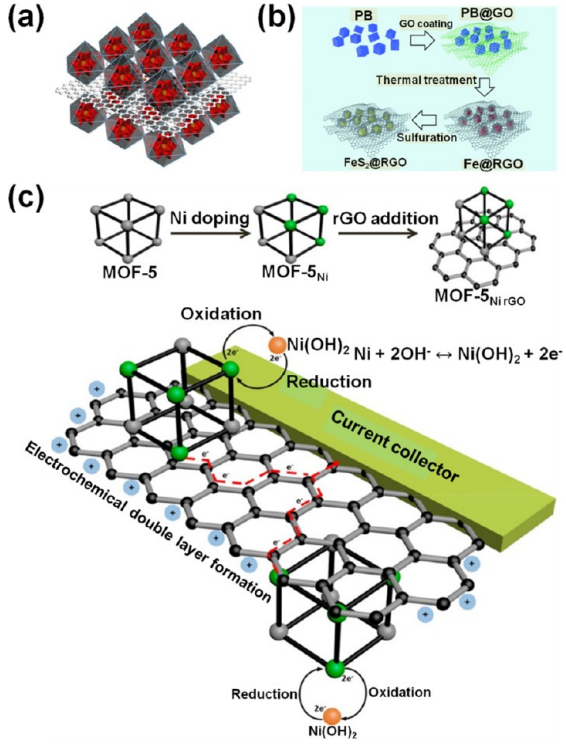

Figure 17. (a) Schematic diagram of POM-based nanocomposites. Reproduced with permission from ref 113. Copyright 2018 Elsevier. (b) Schematic of the synthesis process of FeS_2@RGO. Reproduced with permission from ref 114. Copyright 2018 Royal Society of Chemistry. (c) Concept for Ni doping and incorporating graphene to form a composite of graphene and Ni-doped MOF-5 and its use as an electrode. Reproduced with permission from ref 115. Copyright 2015 American Chemical Society.

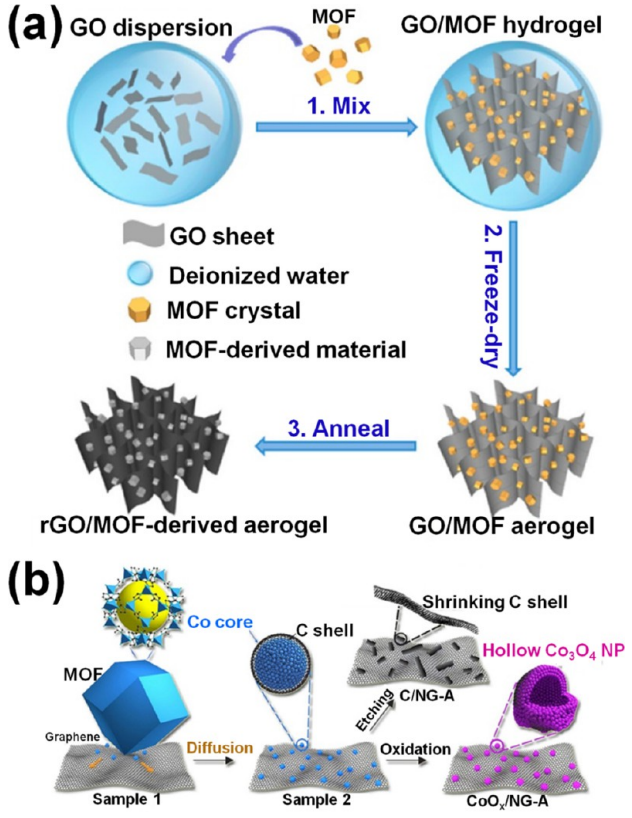

Figure 18. (a) Preparation processes for graphene oxide/MOF- and graphene/MOF-derived composite aerogels. Reproduced with permission from ref 116. Copyright 2017 American Chemical Society. (b) Schematic of the formation process of CoO_x/N-doped graphene aerogels and C/N-doped graphene aerogels. Reproduced with permission from ref 117. Copyright 2017 American Chemical Society.

Co_3O_4 composite product (Figure 10b).[77] When this composite material was inserted into the anode of a lithium-ion battery, excellent electrochemical performance was maintained, with specific capacities of 813 mA h g^{-1} at 100 mA g^{-1} and 514 mA h g^{-1} at 1000 mA g^{-1}.

Zhou and co-workers fabricated asymmetric supercapacitors by growing the spindle-like α-Fe_2O_3@C on carbon fibers made from nanotubes using MIL-88-Fe (MOF) as a precursor (Figure 10c), which resulted in improved electronic and ionic conductivities relative to those of the simple Fe_2O_3 electrode.[78] The fabricated composite electrode exhibited a high capacitance of 1232.4 mF cm^{-2} at a specific current of 2 mA cm^{-2} as well as a considerable rate performance of 63% capacitance retention when the current density was increased from 2 to 20 mA cm^{-2}. The rooted CNT concept has been also demonstrated by Jiao and co-workers, who prepared a CoP/C@MCNT composite material using a cobalt-based MOF as a template (Figure 11a).[79] The introduction of CNTs significantly improved the capacity values relative to the material without CNTs (547.5 mA h g^{-1} and 190.7 mA h g^{-1}, respectively, at a current density of 500 mA g^{-1} after 200 charge/discharge cycles) despite the observation of smaller electrochemical impedance values, indicating that the rate performance remained constant (Figure 12a).

In addition to rooted CNTs, CNTs can also be used as promising support materials for growing MOFs. For example, He and co-workers demonstrated this concept by growing a V-based MOF on CNT fibers (Figure 11b) to yield a binder-free electrode material that exhibited a 50-fold increase in current density with a capacity retention of 64.3%.[80] Tang and co-workers synthesized a CNT-supported ternary metal oxide ($ZnCo_2O_4$) to obtain superior anode materials for lithium-ion batteries.[81] In this study, the authors grew MOF precursors on the highly conductive CNT supports, followed by post-heat treatment (Figure 11c), which led to the formation of a composite material that exhibited a desirable capacity value of 1507 mA h g^{-1} at a current density of 100 mA g^{-1} after 200 cycles of repeated charge/discharge cycles (Figure 12b).

2.2.2. In Situ Grown CNT Supports. As an alternative method to the introduced or inserted CNTs discussed in the previous section, some metal species can serve as seeds for *in situ* grown CNT supports when exposed to a continuous supply of carbon. Due to the well-ordered atomic arrangement of metal species that serve as seeds for nucleation, these *in situ* grown supports may yield composite systems with better bridging effects relative to those formed via inserted CNTs due to the greater degree of chemical bonding that can form during the former process. Tabassum and co-workers synthesized a B/N-codoped, CNT-encapsulated, cobalt phosphide material derived from a MOF precursor for use in electrochemical hydrogen evolution reactions at all pH values.[82] The CNT in this study plays two main roles: (i) it acts as a support material to protect the cobalt phosphide nanoparticles from agglomeration, and (ii) it behaves as an active material to synergistically improve the hydrogen revolution reaction.

https://dx.doi.org/10.1021/acsanm.0c00702
ACS Appl. Nano Mater. 2020, 3, 3964−3990

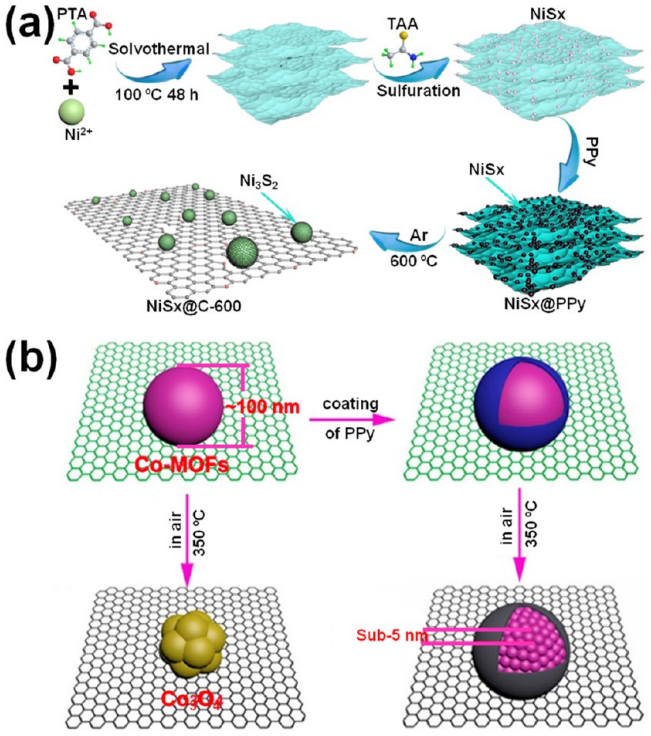

Figure 19. (a) Schematic diagram of the fabrication of NiS_x@C-600. Reproduced with permission from ref 118. Copyright 2019 Elsevier. (b) Schematic illustration of the spatially confined pulverization process. Reproduced with permission from ref 122. Copyright 2018 American Chemical Society.

Gao and co-workers synthesized a CNT-supported carbon polyhedron derived from ZIF-67 (Figure 13a) that exhibited a high capacitance of 343 F g^{-1} when used as an electrode for electrochemical supercapacitors.[83] The improved performance for this composite material is attributed to the rich space (171.6 m^2 g^{-1}) and short ion diffusion pathways (mesopores and micropores, ~0.2 cm^3 g^{-1}). Additionally, highly conductive CNT scaffolds can also be formed by using a Co-containing MOF as precursors. For example, Xiong and co-workers demonstrated the rapid, facile intercalation of K^+ ions in CNTs derived from the pyrolysis of cobalt-containing MOFs, suggesting the feasibility of using an electrode for K^+ ion storage.[84] A similar *in situ* grown CNT method has been studied by Lei and co-workers in which a Zn/Co-based zeolitic imidazolate framework was used as a precursor, and following a heat treatment process, the CNT was *in situ* rooted, owing to the existence of cobalt species.[85] Finally, sulfuration conduction formed the final CoS_2 product (Figure 13b), leading to a composite anode material that exhibited high capacitance (635.8 F g^{-1} at 1 A g^{-1}), suitable rate performance (544.2 F g^{-1} at 10 A g^{-1}), and long-term cycling stability (88.0% retained after 2000 cycles).

CNTs have been demonstrated to be an important type of support material with many attractive advantages; however, some disadvantages exist, such as the aggregation of CNTs and the difficulty of manufacturing electrodes that necessitates the use of binders. In this context, aggregation is unique from the agglomeration of active materials loaded on the CNT tubes. Although CNTs can effectively separate the MOF or MOF-derivative particles, as discussed above, the small size of CNTs (dozens of nanometers) generally aggregate to a larger bulk form after the products are dried. As such, the aggregation of CNTs remains the more significant drawback relative to the difficulties encountered during the physical preparation of the electrodes using the CNT-supported MOF or MOF derivative powers, and the issue of aggregation will have to be solved for CNT-based composite systems to find use in commercial applications.

2.3. Graphene. Graphene, a robust, two-dimensional material comprised of a monolayer of sp^2-hybridized carbon, exhibits excellent conductivity and has been regarded as a potential candidate for use in support materials. In recent years, a significant number of graphene-supported MOF composite materials have been reported for use in electrodes.[86−102] Importantly, the graphene support is able to disperse

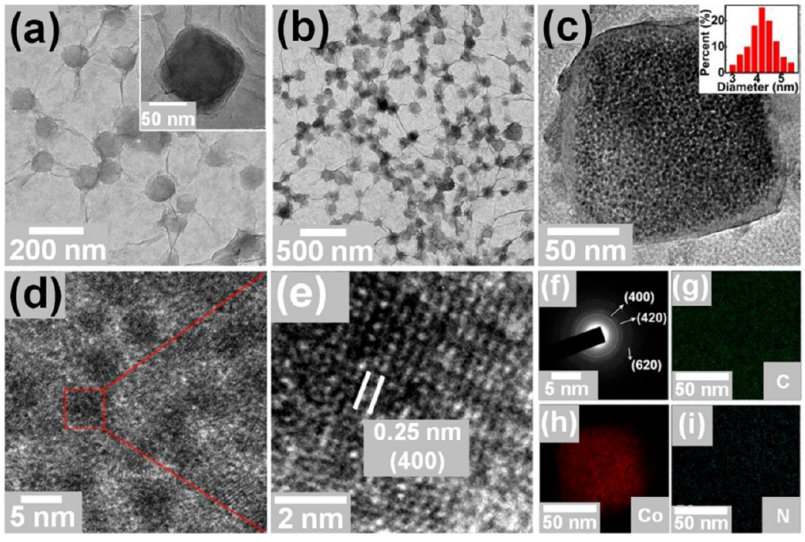

Figure 20. (a) TEM images of GO/Co-MOFs/polypyrrole and (b) Co-MOF nanocrystals encapsulated in N-doped carbon/graphene at 350 °C. (c,d) HRTEM images of Co-MOF nanocrystals encapsulated in N-doped carbon/graphene at 350 °C. The inset shows a histogram of the size distribution of nanocrystals. (e) The corresponding lattice structure, (f) selected area diffraction pattern, and (g−i) element mapping images. Reproduced with permission from ref 122. Copyright 2018 American Chemical Society.

https://dx.doi.org/10.1021/acsanm.0c00702
ACS Appl. Nano Mater. 2020, 3, 3964−3990

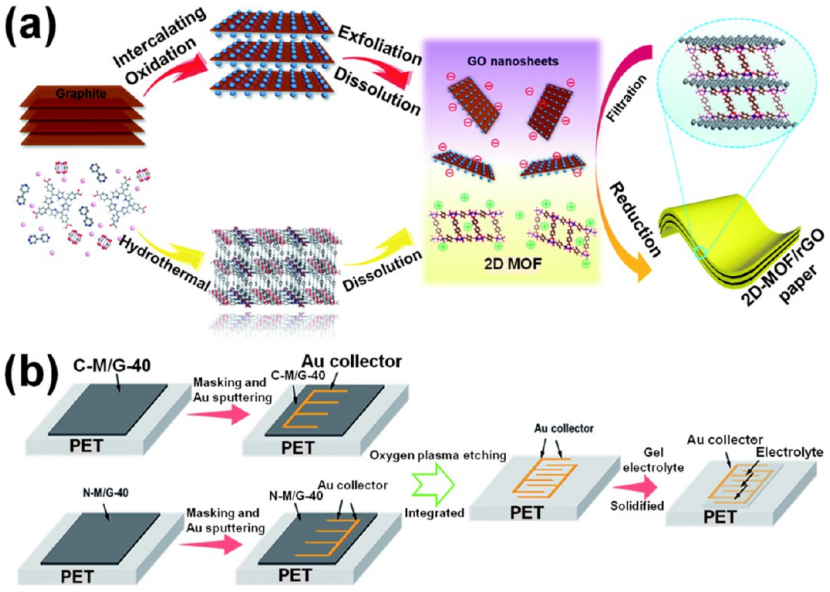

Figure 21. (a) Schematic of fabrication of the flexible two-dimensional MOF/graphene hybrid papers through an electrostatic self-assembly route. (b) Schematic of the process of the preparation of Co-MOF/graphene−40%//Ni-MOF/graphene−40% asymmetric microsupercapacitor devices on a substrate. Reproduced with permission from ref 124. Copyright 2018 Royal Society of Chemistry.

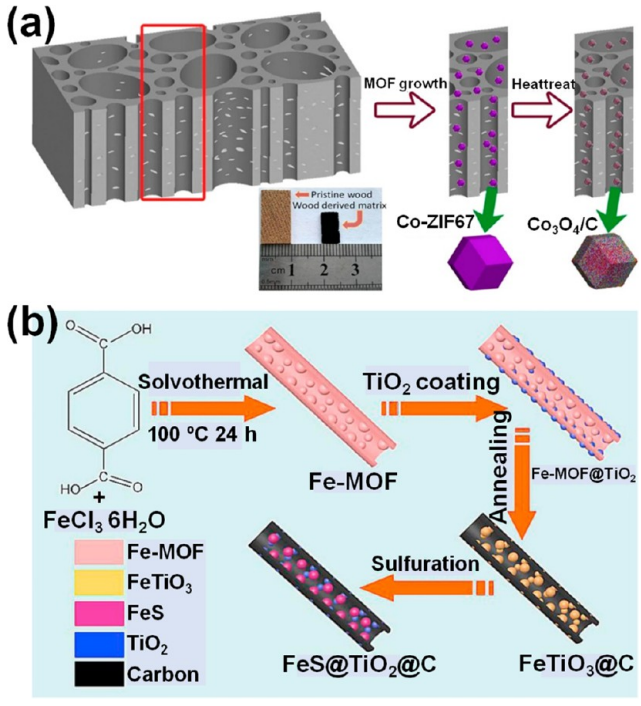

Figure 22. (a) Schematic diagram of the preparation of Co_3O_4/C-modified wood substrates. Reproduced with permission from ref 125. Copyright 2012 Royal Society of Chemistry. (b) Schematic illustration of the detail preparation processes of uniform ternary FeS@TiO_2@C nanotubes derived from a facilely prepared Fe-MOF precursor. Reproduced with permission from ref 126. Copyright 2019 Elsevier.

the MOF (or MOF derivative) while physically bridging them, resulting in improved stability and conductivity when the composite material is employed in an electrode; as such, we have summarized the design methods and principles for graphene-supported MOF electrode materials in this section.

Rajpurohit and co-authors synthesized a graphene-supported, bimetallic Cu- and Fe-based MOF and studied the electrochemical performance of this composite material when it was used as an electrode material for a symmetric capacitor.[103−107] In this report, the benefit from incorporating the highly conductive graphene support is evident from the greater retention of initial capacitance values (78.4 and 69.0% at current density of 5.0 A g^{-1} for the materials with and without graphene, respectively) as well as from the high power density of 26973.13 W kg^{-1} (Figure 14a).

A common design concept employed to incorporate the two-dimensional graphene support involves a sandwich-structured composite electrode in which the graphene and active materials are integrated in layers. For example, Yu and co-workers developed a sandwich-type composite electrode material by using one precursor for the preparation of both anode and cathode materials, as shown in Figure 15a and found the material exhibited exceptional energy storage performances.[108] In this material design concept, the graphene sheets display a dual functional feature in which they disperse the MOF particles, and the MOF particles separate the graphene sheets to simultaneously obtain electrolyte infiltration and electronic flow throughout the electrode material.

Similar to rooted CNTs, graphene supports can also be rooted into the final electrode materials through the growth of MOFs directly onto graphene sheets. For example, Zhou and co-workers demonstrated this concept by fabricating Ni-MOFs on graphene supports, resulting in the formation of a GO@MOF structure (Figure 15b) that exhibits excellent electrochemical performances, including a long-term operational lifetime (3000 consecutive charge/discharge cycles), a good rate performance (85% of capacitance retention when current density increased from 1 to 10 A g^{-1}), and a high capacitance (2192.4 F g^{-1} at a current density of 1 A g^{-1}).[109] Zheng and co-workers further demonstrated this concept by forming a graphene-wrapped, bimetallic Co−Ni MOF as a cathode material for Zn−air batteries (Figure 15c).[110] The authors emphasized the synergistic effect between the graphene

https://dx.doi.org/10.1021/acsanm.0c00702
ACS Appl. Nano Mater. 2020, 3, 3964−3990

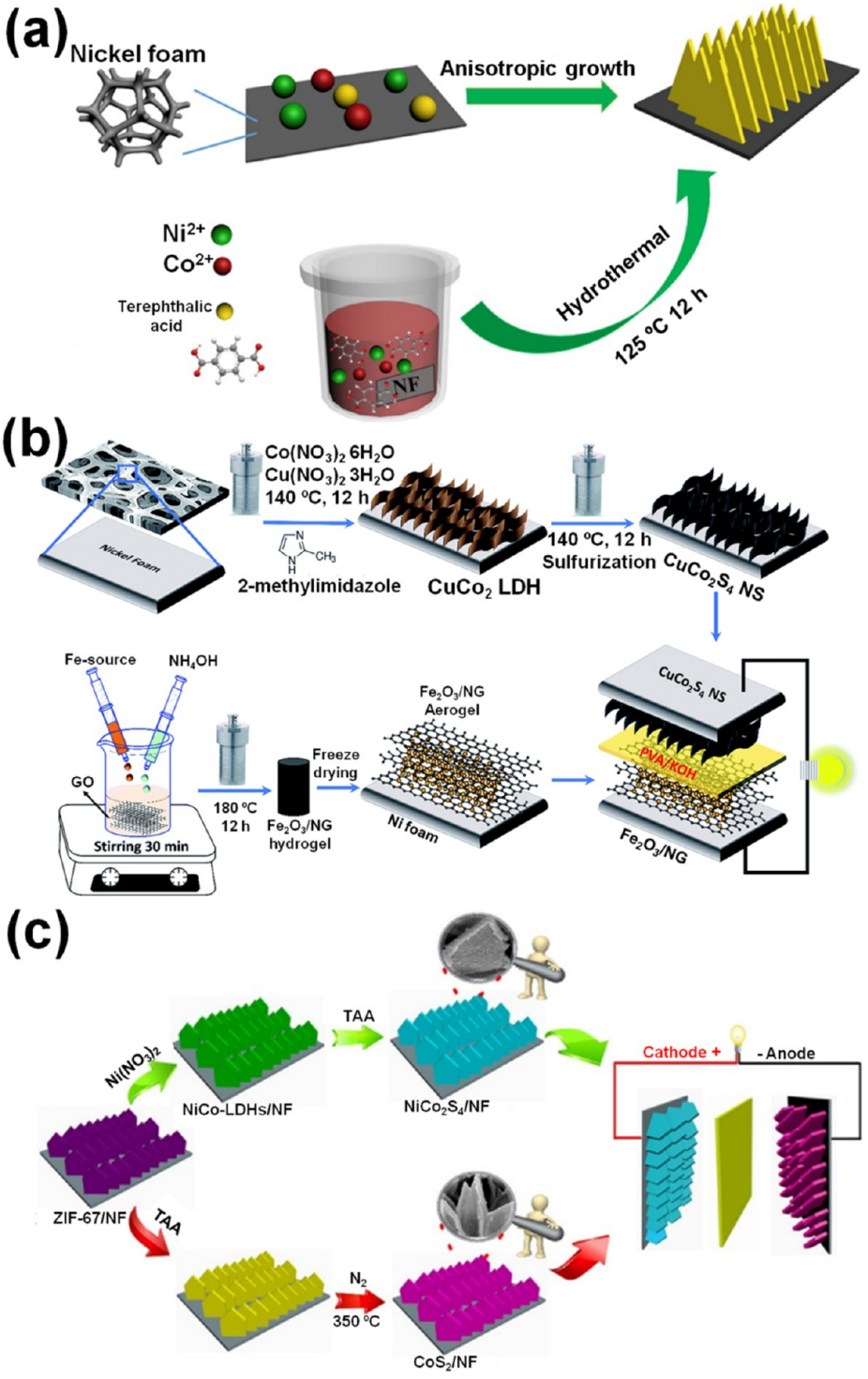

Figure 23. (a) Schematic illustration of the formation of NiCo-MOF nanosheet arrays on nickel foam. Reproduced with permission from ref 131. Copyright 2019 Elsevier. (b) Schematic illustration of the design and fabrication of the $CuCo_2S_4$ nanosheets and Fe_2O_3/nitrogen-doped graphene aerogel and their application in all solid-state asymmetric supercapacitors. Reproduced with permission from ref 132. Copyright 2019 Royal Society of Chemistry. (c) Schematic illustration of the synthesis process of the composite and fabrication of the asymmetric supercapacitor. Reproduced with permission from ref 133. Copyright 2018 American Chemical Society.

support and MOFs in which the graphene wrapping layers serve as electronic pathways, and the MOFs provide the active sites, resulting in great performance when employed in electrochemical reactions. In a similar strategy, Wang and co-workers synthesized a sandwich-type graphene/porous carbon electrode material that was formed following an acid wash of a MOF-5 precursor (Figure 16a), leading to an improvement in both charge (0.26 Ω) and mass transfer properties (relaxation time constant value of 215 ms with a right shifted frequency at a −45° phase angle in Bode curves), even at the high scan rate of 5 V s^{-1} (Figure 14b).[111] Similar sandwich-structured materials can also be formed using graphene supports and

https://dx.doi.org/10.1021/acsanm.0c00702
ACS Appl. Nano Mater. 2020, 3, 3964−3990

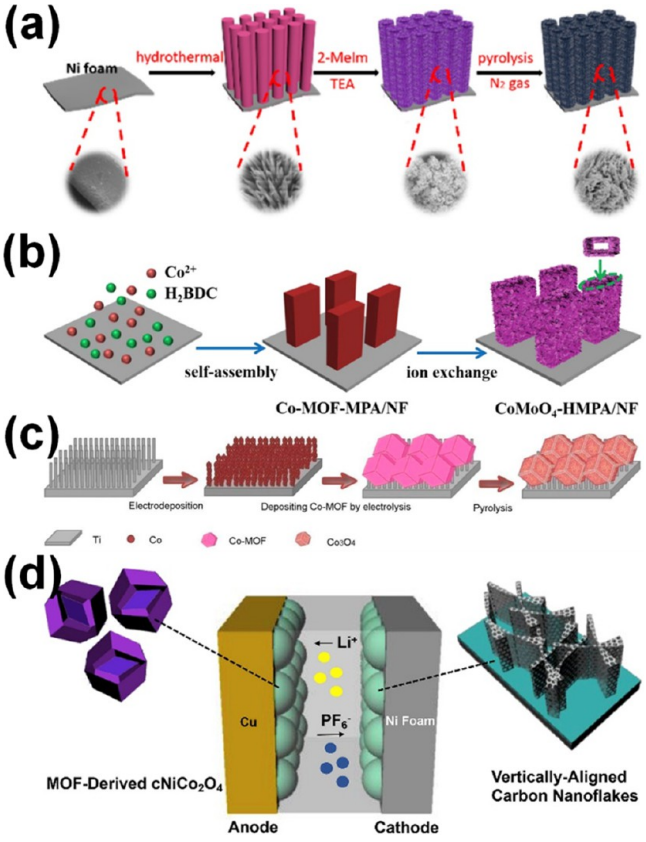

Figure 24. (a) Illustration of the fabrication of Co_3O_4−carbon nanowires on Ni foam. Reproduced with permission from ref 134. Copyright 2017 American Chemical Society. (b) Schematic illustration of the synthesis of $CoMoO_4$−hollow microplate array on Ni foam. Reproduced with permission from ref 135. Copyright 2019 Elsevier. (c) Schematic diagram of preparing Co-MOF-derived Co_3O_4 on Ti nanowire arrays. Reproduced with permission from ref 136. Copyright 2018 Elsevier. (d) Schematic illustration for the design of the Li-ion capacitor. Reproduced with permission from ref 138. Copyright 2019 Elsevier.

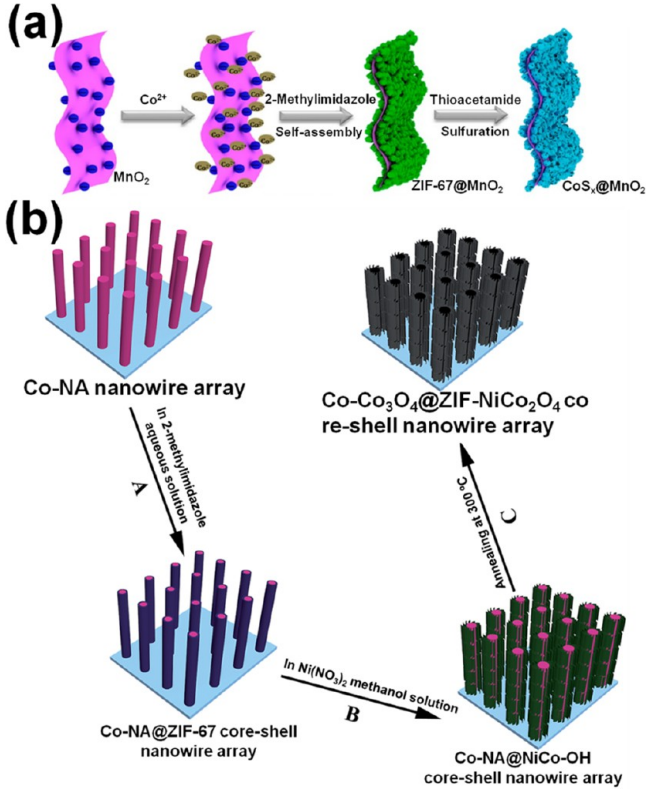

Figure 25. (a) Schematic synthesis of CoS_x@MnO_2. Reproduced with permission from ref 139. Copyright 2017 American Chemical Society. (b) Schematic illustration of the fabrication process of a Co−Co_3O_4@ZIF−$NiCo_2O_4$ core−shell nanowire array electrode on Ni foam. Reproduced with permission from ref 146. Copyright 2016 Royal Society of Chemistry.

other compounds for energy storage applications, as shown in previous reports (Figure 16b and 17a and b).[112−114] In these studies, improvements in electrochemical performance, such as capacity and conductivity, are observed following the introduction of graphene into the electrodes.

Another effective method used to increase the redox activity of the electrode material involves the synergetic activation in which the performance of the composite material exceeds the sum of each individual component. For example, Banerjee and co-workers prepared a composite electrode material consisting of a redox-active Ni-doped MOF and graphene sheets.[115] This composite material exhibited a high capacitance value of 240 F g^{-1}, which was more than the sum of the parts, by incorporating a Faradaic redox reaction (one-electron transfer) between NiO−(OH) and $Ni(OH)_2$ (Figure 17c). Xu and co-workers demonstrated a facile strategy for synthesizing an aerogel using graphene/MOF composites as precursors.[116] This preparation method can be conducted rapidly (within several minutes) to yield materials with well-controlled compositions (Figure 18a).

Similarly, Xia and co-workers fabricated monodispersed metal oxides and porous carbon materials in which the graphene aerogel-assisted method was used together with the Co-based MOF precursor (Figure 18b).[117] Shuang and co-workers demonstrated a composite electrode material that is carbon shell-confined in which a Ni-based MOF was used as a precursor, followed by a carbonization process (Figure 19a).[118] The best rate performance was obtained by the small Ni_3S_2 nanoparticles (~15.9 nm) confined within the carbon shell, suggesting the small particle size is crucial for shortening the ionic and electronic pathways during electrochemical reactions.[119−121] While the use of support materials can help mitigate losses in performance arising from longer ionic/electronic pathways, the best performance is generally observed when the active materials are less than 10 nm in size. Xiao and co-workers reported the synthesis of an ultrasmall (less than 5 nm), graphene-supported, Co-based MOF.[122] In this innovative design (Figure 19b), the authors improved the decomposition temperature for the Co-based MOF by coating a polymer on the surface; after heating this material at 350 °C, the Co-based MOF would collapse rather than being oxidized. Using this strategy, active materials with a significantly smaller size can be obtained (Figure 20). In addition to the stacking of graphene layers that has been observed during the preparation of electrode materials, graphene sheets can also be used as wrapping layers. For example, Cao and co-workers demonstrated this wrapping concept using graphene and a one-dimensional Mo-based MOF in which the wrapping was achieved by stirring a mixture of the graphene precursor and the MOF.[123] When this composite material was used as an electrode in a supercapacitor, an excellent rate capability (~61% of the capacity

https://dx.doi.org/10.1021/acsanm.0c00702
ACS Appl. Nano Mater. 2020, 3, 3964−3990

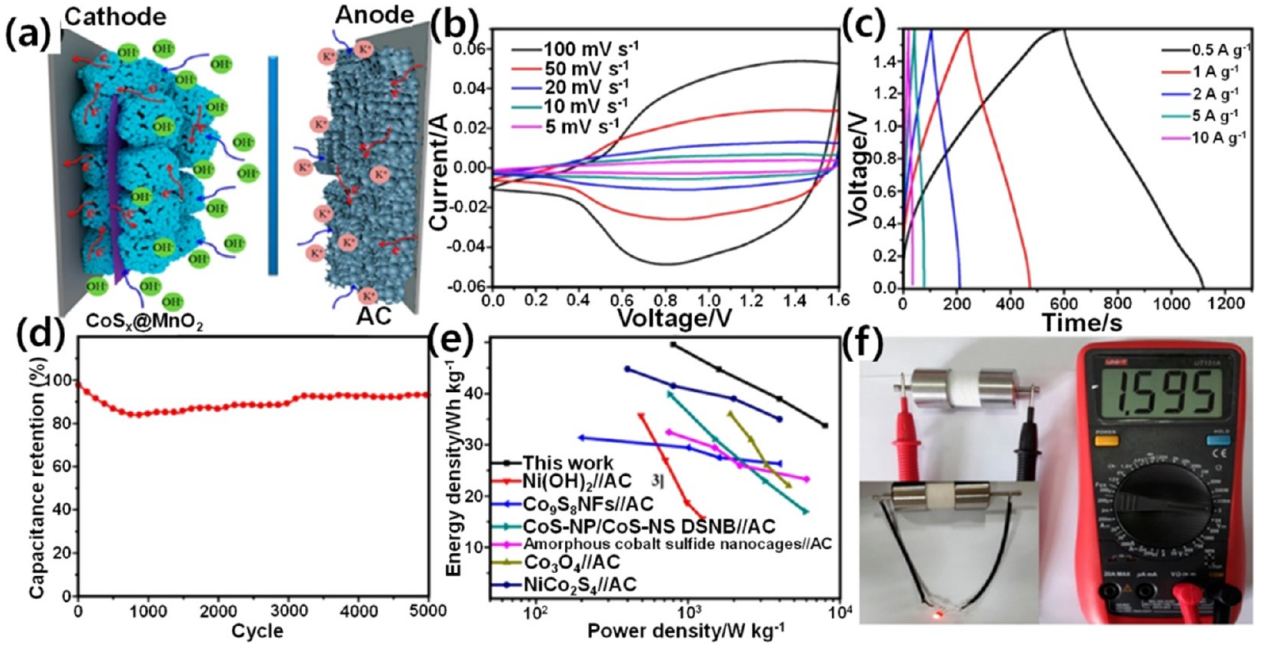

Figure 26. (a) Charge-storage mechanism of the $CoS_x@MnO_2$ cathode and the activated carbon anode in the hybrid supercapacitors system. (b) CV curves at different scan rates and (c) charging−discharging curves at different current densities of the hybrid supercapacitors. (d) Cyclic stability of the hybrid system at 5 A g^{-1}. (e) Ragone plot of the $CoS_x@MnO_2$//AC hybrid supercapacitors and related reports elsewhere. (f) Digital image of the hybrid supercapacitor's cell voltage and the inset of a red-light-emitting diode lighted by the hybrid supercapacitor device. Reproduced with permission from ref 139. Copyright 2012 American Chemistry Socieity.

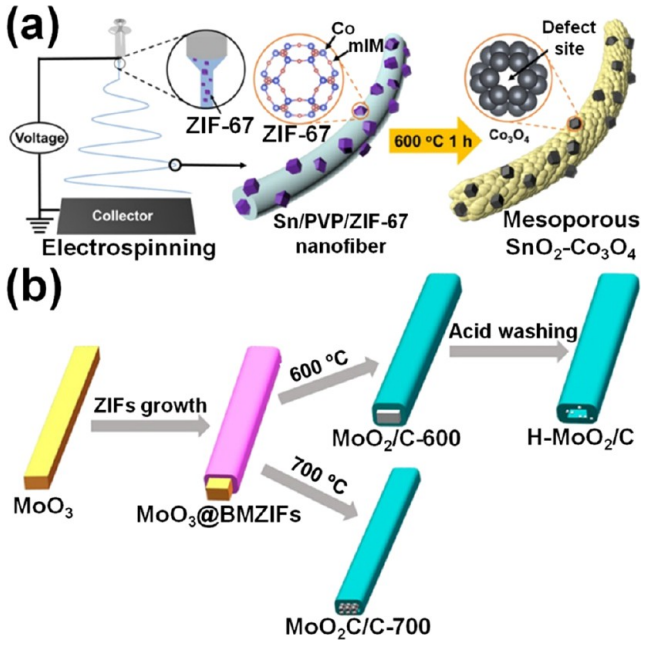

Figure 27. (a) Schematic illustration of the synthesis process of SnO_2−Co_3O_4 nanofibers. Reproduced with permission from ref 147. Copyright 2012 American Chemical Society. (b) Schematic illustration for the synthetic procedure of carbon-coated Mo-based composites. Reproduced with permission from ref 148. Copyright 2012 American Chemical Society.

remained when the current density increased from 1 to 10 A g^{-1}) and a long cycle life (~87.5% of the capacity remained after 6000 charge/discharge cycles at 6 A g^{-1}) were observed, potentially resulting from the graphene wrapping layers providing good electronic conductivity and inhibiting aggregation of the MoO_3 active material.

Overall, graphene has been widely used as a two-dimensional support material due to its good inherent conductivity as well as its high flexibility that enables the fabrication of foldable devices. Despite these advantages, however, the two main disadvantages regarding graphene-based support materials include graphene lamination and graphene oxidation prevention difficulty. The use of stacked graphene offsets the advantages gained from the implementation of separated MOFs and MOF derivatives on graphene, significantly reducing the anticipated benefits from using graphene. Additionally, the susceptibility of graphene to oxidation necessitates an activation process conducted by heating the substrate under a reducing or inert gas flow at around 300 °C, which increases the manufacturing costs and limits the use of graphene in practical applications. Thus, more consideration should be given to these key factors to facilitate the development of advanced, but practical, electrode materials.

2.3.1. Mechanistic Considerations. In addition to excellent conductivity, graphene sheets also exhibit robust mechanical properties. For example, Cheng and co-workers fabricated high-strength, flexible, and two-dimensional MOF/graphene paper-type electrodes (Figure 21a) that demonstrate a tensile strength of 89.9 MPa and a Young's modulus of 34.4 GPa; importantly, the significant structural integrity observed for this material originates from the presence of graphene due to the synergistic effect between the reduced graphene oxide (rGO) and the two-dimensional MOF sheets via both electrostatic forces and van der Waals forces.[124] Furthermore, a micro-supercapacitor was fabricated using this paper-type electrode (Figure 21b), suggesting a variety of devices can potentially benefit from the use of graphene supports.

2.4. Other Carbon Supports. In addition to the well-known CNTs and graphene sheets, other carbon-derived materials have been studied for use as bridges for both MOFs and MOF derivatives. For example, Zhao and co-workers

https://dx.doi.org/10.1021/acsanm.0c00702
ACS Appl. Nano Mater. 2020, 3, 3964−3990

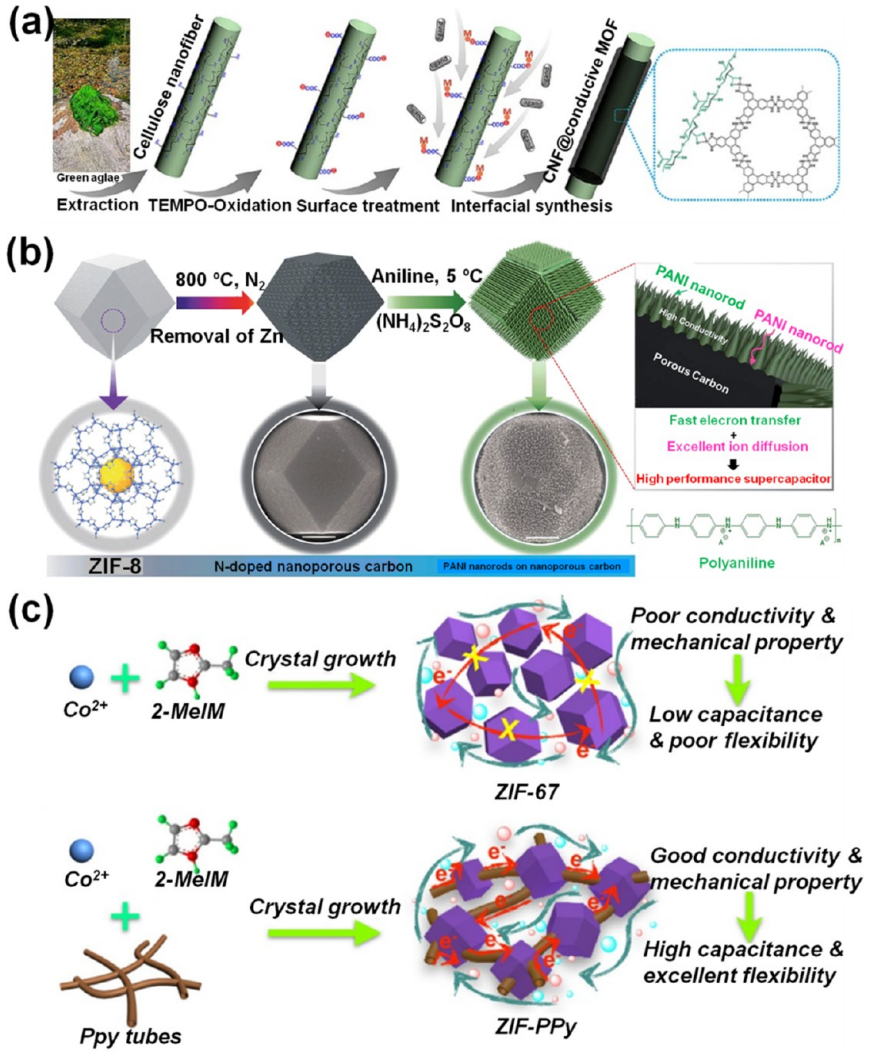

Figure 28. (a) Schematic of the synthesis procedure for CNF@c-MOF hybrid nanofibers. Reproduced with permission from ref 154. Copyright 2012 American Chemical Society. (b) Schematic illustration of the synthetic process for the attainment of nanoporous carbon−polyaniline core−shell nanocomposite materials. Reproduced with permission from ref 155. Copyright 2012 Royal Society of Chemistry. (c) Schematic illustration of the procedure for the fabrication of ZIF-67 and ZIF-polypyrrole. Reproduced with permission from ref 157. Copyright 2012 American Chemical Society.

demonstrated this concept by using a channel-rich carbon support that is derived from wood (Figure 22a).[125] Loading the Co-based, MOF-derived Co_3O_4 on the surface of this carbon support results in a composite material that features ultrafast mass transport properties resulting from rich tunnels formed by the wood vessels as well as a uniform reaction interface formed by the homogeneous dispersion of the Co_3O_4/C active material. Similarly, Xu and co-workers demonstrated the use of a carbon tube derived from an Fe-based MOF, a protected dual phase (FeS and TiO_2) anode material for use in sodium-ion batteries (Figure 22b).[126] In this study, multiple benefits of the carbon tubes were apparent, such as the mitigation of volume changes during battery operation as well as an increase in both the ionic and electronic conductivities, all of which result in improved rate and cycling performances. For example, the carbon tube-containing sample exhibited a 26% greater capacity retention relative to that of the control when the current density was increased from 0.1 to 5 A g^{-1}, and the composite material containing carbon tubes demonstrated significantly better cycling performance in comparison to the noncarbon tube sample after 150 cycles (444 and 384 mA h g^{-1}, respectively).

2.5. Metal supports. In addition to carbon-based support materials, metallic supports have also been demonstrated to be competent bridging materials. Several recent reports have detailed the growth of MOFs and MOF derivatives on metal surfaces, such as Ni or Cu foams, to improve the performance when these composites are employed in supercapacitors and other electrochemical applications.[127−130] In another example, Wang and co-workers synthesized nickel foam-supported MOF nanoarrays (Figure 23a), and this material demonstrates an excellent capacitance value of 2230 F g^{-1} at a current density of 1 A g^{-1}, which is a significant improvement relative to the capacitance values for many previously reported electrode materials. Importantly, the superior electrochemical performance of this composite material was attributed to the well-aligned MOF nanosheets in addition to the excellent electronic contact that is achieved through the use of the metallic nickel foam support.[131]

Similarly, Bahaa and co-workers reported nickel foam-connected $CuCo_2S_4$ nanosheets through a two-step method

https://dx.doi.org/10.1021/acsanm.0c00702
ACS Appl. Nano Mater. 2020, 3, 3964−3990

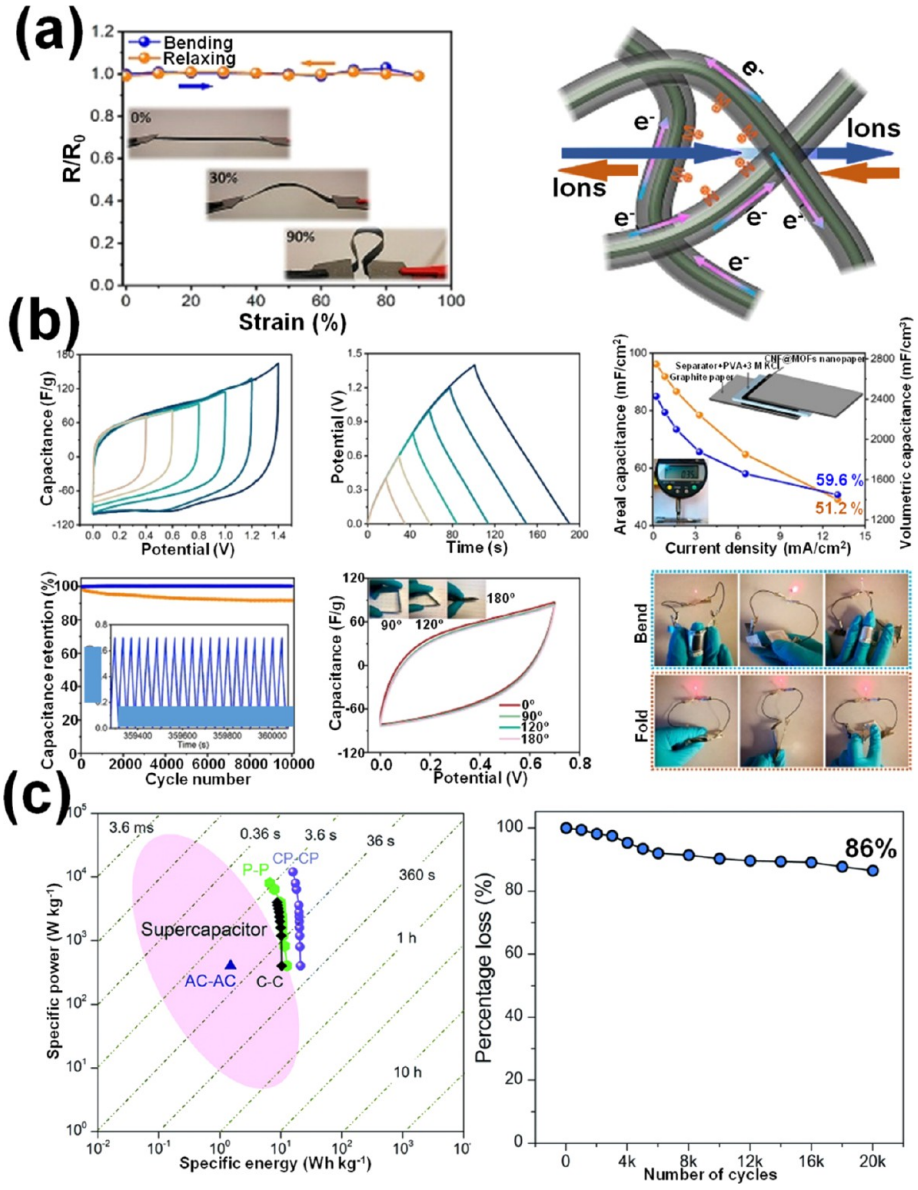

Figure 29. (a) Normalized resistance of CNF@Ni-2,3,6,7,10,11-hexaiminotriphenylene nanopaper at different bending states; schematic diagram showing the charge transfer and electrolyte ion transport. (b) Electrochemical performances of the CNF@Ni-2,3,6,7,10,11-hexaiminotriphenylene double-layer supercapacitor: cyclic voltammetry curves, galvanostatic charge and discharge curves, calculated areal capacitances, cyclic performance and capacitance retention data, cyclic voltammetry curves, and photograph of LED powered by the devices. Reproduced with permission from ref 154. Copyright 2012 American Chemical Society. (c) Electrochemical performances: Ragone plot for symmetric supercapacitors and long-term cycling performance. Reproduced with permission from ref 155. Copyright 2012 Royal Society of Chemistry.

using Co- and Cu-based MOFs as precursors (Figure 23b).[132] In this study, the fabricated electrode material exhibited a good capacity and a rate performance with a 77.9% capacity retention after increasing the current density from 3 to 50 mA cm^{-2}. By employing a similar strategy and using nickel foam as a support material, Guo and co-workers also fabricated metal sulfide flakes derived from ZIF-67 (Figure 23c).[133] In this report, the authors emphasized the use of a highly conductive matrix for improving the mass and electron transfer as well as shortening the charge and ion diffusion path. The superior bridge material, nickel foam, has also been demonstrated in many other reports, such as nickel foam-supported Co_3O_4−C nanowire arrays and hollow $CoMoO_4$ microplate arrays (Figure 24a and b).[134,135]

Metal nanowires comprise another class of support materials that exhibit good electronic conductivity. Zhao and co-workers prepared a Ti nanowire-supported, Co-based MOF through an electrochemically assisted method, resulting in a composite electrode that demonstrates both a high capacity of 700 mA h g^{-1} at a specific current of 1.0 A g^{-1} as well as an excellent rate performance of 300 mA h g^{-1} at a current density of 20 A g^{-1}, owing to the well-dispersed and strongly adhered active materials on the Ti wire supports (Figure 24c).[136] Similarly, Hong and co-workers synthesized a composite material comprised of Ni wire-supported Bibased MOF sheets for supercapacitor applications.[137] The as-prepared Ni@CoNi-MOF electrode imparts an excellent rate performance (325 C cm^{-3}) at a current density of 5 A cm^{-3}, while maintaining the specific capacity of 813 C cm^{-3} at a current density of 0.5 A

https://dx.doi.org/10.1021/acsanm.0c00702
ACS Appl. Nano Mater. 2020, 3, 3964−3990

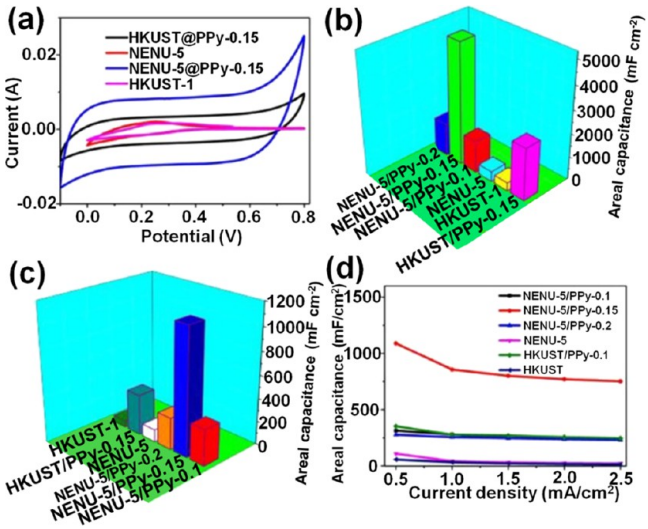

Figure 30. Electrochemical performances: (a) CV curves, (b) maximum areal capacitances, (c) areal capacitances, and (d) calculated areal capacitances. Reproduced with permission from ref 157. Copyright 2012 American Chemical Society.

cm^{-3}. Finally, Cheng and co-workers fabricated lithium-ion capacitors using nickel foam-supported vertically aligned carbon nanoflakes as the cathode and copper-supported MOF-derived $NiCo_2O_4$ as the anode (Figure 24d).[138] Importantly, this hybrid lithium-ion capacitor displayed a high rate performance of 40 kW kg^{-1} while having an energy density of 26.44 W h kg^{-1}.

2.6. Metal Oxide Supports. In addition to pure metals, well-shaped metal oxides have also been used as support or bridging materials for both MOFs and MOF derivatives. Generally, metal oxides are used as active materials for electrochemical applications, and based on previous reports, metal oxides have also demonstrated significant potential for use as anode materials in lithium-ion batteries. Therefore, metal oxides that are incorporated with the other active materials may potentially serve as both the active and support materials, and as a result, both the metal oxides and MOFs or MOF derivatives should be treated as active materials in the context of specific capacity calculations. Therefore, more attention should be paid on this factor. Similar to the other aforementioned support materials, the incorporation of structured metal oxides with MOFs (and MOF derivatives) has been shown to effectively disperse the MOF-based active materials, resulting in superior electrolyte infiltration. In this section, we have summarized the metal oxide-supported MOFs and MOF-derived composite materials for use in electrochemical applications.

Chen and co-workers reported a graphene-like MnO_2 sheet used as a support for a MOF-derived hollow cobalt sulfide

Table 1. Comparison of Electrochemical Performance for the CNF-Supported MOFs or MOF Derivatives

entry	materials	capacity/capacitance	current density	reference
1	MnO_2 and Bi_2O_3 flakes/CNF	124.8 μW h cm^{-2}	2.55 mW cm^{-2}	49
2	NiCo-P/NiCo−OH	1100 F g^{-1}	100 F g^{-1}	50
3	Co_3O_4/nanoporous carbon	1.22 F cm^{-2}	0.5 mA cm^{-2}	54
4	PANI−ZIF-67−CNF	2146 mF cm^{-2}	10 mV s^{-1}	58
5	CNFs/porous $CoSe_2$	713.9 F g^{-1}	1 mA cm^{-2}	65
6	$NiCo_2O_4$ nanosheets/ZnO@C/CNF	2650 F g^{-1}	5 A g^{-1}	66
7	CoS_2/porous CNF	876 mA h g^{-1}	100 mA g^{-1}	67
8	MoS_2 nanosheets@N−C nanowall/CNF	619.2 mA h g^{-1}	200 mA g^{-1}	68
9	CNT-porous C	75.1 F g^{-1}	1 A g^{-1}	71
10	$CoSe_2$@C/CNTs	404 mA h g^{-1}	0.2 A g^{-1}	76
11	CNT/Co_3O_4	813 mA h g^{-1}	100 mA g^{-1}	77
12	spindle-like α-Fe_2O_3@C	1232.4 mF cm^{-2}	2 mA cm^{-2}	78
13	CoP/C@MCNT	547.5 mA h g^{-1}	500 mA g^{-1}	79
14	CNT/$ZnCo_2O_4$	1507 mA h g^{-1}	100 mA g^{-1}	81
15	CoS_2/CNT	635.8 F g^{-1}	1 A g^{-1}	85
16	GO@Ni-MOF	2192.4 F g^{-1}	1 A g^{-1}	109
17	FeS/TiO_2/CNT	444 mA h g^{-1}	0.1 A g^{-1}	126
18	FeS/TiO_2/CNT	384 mA h g^{-1}	5 A g^{-1}	
19	nickel foam-supported MOF nanoarrays	2230 F g^{-1}	1 A g^{-1}	131
20	Ti nanowire/Co-MOF	700 mA h g-1	1.0 A g-1	136
21	Ti nanowire/Co-MOF	300 mA h g^{-1}	20 A g^{-1}	
22	Ni@CoNi-MOF	325 C cm^{-3}	5 A cm^{-3}	137
23	Ni@CoNi-MOF	813 C cm^{-3}	0.5 A cm^{-3}	
24	nickel foam/carbon nanoflakes	26.44 W h kg^{-1}	40 kW kg^{-1}	138
25	MnO_2 sheet/hollow cobalt sulfide	1635 F g^{-1}	1 A g^{-1}	146
26	Co_3O_4 nanowire/$NiCo_2O_4$ nanoflakes	30.2 W h kg^{-1}	11.1 kW kg^{-1}	
27	SnO_2−Co_3O_4 nanofiber	1287 mA h g^{-1}	500 mA g^{-1}	147
28	polyaniline nanorods/porous carbon	21 W h kg^{-1}	12 kW kg^{1-}	155
29	polypyrrole coated polyoxometalate-based MOF	5147 mF cm^{-2}	same current density	156
	polyoxometalate-based MOF	432 mF cm^{-2}		
30	polypyrrole/ZIF-based MOF	597.6 F g^{-1}	same current density	157
	ZIF-based MOF	99.2 F g^{-1}		

https://dx.doi.org/10.1021/acsanm.0c00702
ACS Appl. Nano Mater. 2020, 3, 3964−3990

material (Figure 25a).[139−145] Importantly, this composite electrode material exhibited excellent electrochemical performances, including the capacitance values (1635 F g^{-1} at a current density of 1 A g^{-1}), rate performance (71% capacitance retention when current density increased from 1 to 10 A g^{-1}), and lifespan (5000 cycles with 80% of capacitance retention, Figure 26), that result from the MnO_2 sheets favorably directing the active material particles. In addition to two-dimensional metal oxide supports, wire-type metal oxide supports comprise another class of potential candidates. For example, Yu and co-workers synthesized Co_3O_4 nanowire-supported $NiCo_2O_4$ nanoflakes with core−shell structures (Figure 25b), and similar to other one-dimensional support materials, this design results in electrodes that exhibit fast charge transfer and ion diffusion properties (maintaining 30.2 W h kg^{-1} at power density of 11.1 kW kg^{-1}).[146]

Similarly, Cheong and co-workers synthesized SnO_2−Co_3O_4 nanofiber supports through the use of ZIF-67 as a template (Figure 27a).[147] Specifically, the Sn-ZIF-67 composite was prepared via an electrospinning method, and upon calcination at 600 °C, the dual metal oxide nanofiber was successfully isolated. The synergetic effect between SnO_2 and Co_3O_4 yielded a composite electrode that exhibited a high capacity of 1287 mA h g^{-1} at 500 mA g^{-1} with a lifetime of 300 repeated charge/discharge cycles. Using a similar strategy, Tian and co-workers used a ZIF-based template to synthesize a molybdenum oxide-based wire-type electrode material.[148] In this study, the ZIF was used to form a carbon shell around the MoO_3 starting material, and the molybdenum oxide/carbon composite nanowire electrodes were isolated following calcination (Figure 27b). When this material was employed as an anode in a lithium-ion battery, high capacity values of 810 and 530 mA h g^{-1} can be obtained for MoO_2/C and Mo_2C/C, respectively, both of which exhibit long lifetimes of up to 600 cycles.

2.7. Conductive Polymer Bridges. Distinct from other bridging materials, conductive polymers represent attractive materials for potentially improving the electronic conductivity of both MOFs and MOF derivatives, as they can provide both structural support and electronic conductivity. In recent years, various polymeric materials have been reported for protecting both MOFs and MOF derivatives as well as optimizing the performance of these composite materials in electrochemical applications.[149−153] In this section, we have selected representative examples in order to discuss this material design strategy.

In one example, Zhou and co-workers fabricated conductive substrates by using cellulose nanofibers, followed by the growth of MOFs on the nanofiber surfaces to yield conductive MOFs, resulting in the formation of free-standing, flexible nanopapers (Figure 28a).[154] When employed as electrode materials for supercapacitors, excellent charge transfer and efficient electrolyte permeation values were achieved, with an electrical conductivity of up to 100 S cm^{-1} (Figure 29a). Furthermore, the prepared supercapacitor provided a suitable long-term cycling stability with a high capacitance retention over 10000 cycles of continuous charge/discharge measurements (Figure 29b).

Using an alternative approach, Salunkhe and co-workers synthesized polyaniline nanorods on a porous carbon matrix derived from ZIF-8 (Figure 28b) and found that a synergetic effect between the organic rods and porous carbon leads to an improvement in supercapacitor performance.[155] The assembled symmetric supercapacitor exhibits the highest energy and power densities of 21 W h kg^{-1} and 12 kW kg^{1-}, respectively, with a high capacity retention of 86% after 20000 cycles (Figure 29c). The use of a conductive polymer can greatly improve the usage rate of active materials, thereby enhancing the performance of these composite materials in the context of electrochemical applications. For example, Wang and co-workers employed a conductive polypyrrole coating layer for a polyoxometalate-based MOF, resulting in a material that exhibits a more than 10-fold improvement in its capacitance value relative to that of the bare MOF material (5147 and 432 mF cm^{-2}, respectively; Figure 30).[156] Finally, Xu and co-workers also employed a conductive polypyrrole backbone to greatly improve the capacitance of a ZIF-based MOF when used as an electrode material in a capacitor (Figure 28c).[157] Specifically, they synthesized a ZIF-based material and incorporated a woven polypyrrole component that can deliver a much higher capacitance of 597.6 F g^{-1} relative to the capacitance value of 99.2 F g^{-1} observed for the bare MOF electrode.

One significant challenge regarding the use of conductive polymers is related to the poor conductivity, relative to metal- and metal oxide-based supports, commonly observed for these materials; however, advances in this context have recently been achieved. One potential strategy that can be used to incorporate polymeric support materials in electrodes consists of a sacrificial concept in which the polymeric material forms a graphitic carbon material that has improved conductivity and ionic diffusion capabilities, which are critical for good rate performances in electrochemical systems. Moving forward, more studies regarding polymer supports are needed to achieve a greater understanding of these supports employed in functional electrode materials.

Recently, some pioneering works on conductive MOFs exhibited potential electrochemical performance when used as electrode materials directly.[158−160] The conductive MOFs can certainly solve the conductivity issue of the normal MOFs. Further development and progress are required for emerging conductive MOFs. The highly conductive MOFs may also become a type of promising electrode materials for use in electrochemical devices. In addition, summarized electrochemical performances of bridged MOFs and MOF derivatives are recorded in Table 1, in which the connected MOFs or MOF derivatives demonstrated superior capacities at higher specific currents. A series of bridging materials consistently suggest the bridging concept for the MOFs and MOF derivatives, highlighting the remaining efforts for the research communities.

3. CONCLUSIONS

In this Review, we have summarized the reported MOF-based heterogeneous electrode nanomaterials for use in electrochemical devices, such as batteries and capacitors, with a focus on the connection, or bridge, between the active nanomaterials. In the absence of a bridging material, MOFs commonly exhibit low conductivities that partially stem from separated nanoparticles; through the integration of a conductive bridging support material, however, composites can be developed that exhibit a more complete utilization of the active nanomaterials, resulting in improvements in desirable electrochemical properties, such as greater electrolyte infiltration and improved rate performances. Furthermore, the decay of the electrochemcial performance over long-term use is another disadvantage, which

https://dx.doi.org/10.1021/acsanm.0c00702
ACS Appl. Nano Mater. 2020, 3, 3964−3990

is mainly attributed to the loss and decomposition of the active materials. The integrity of single MOFs and MOF derivatives with supporting materials is able to suppress the loss of active materials, thereby prolonging the lifetime of devices. We focused our discussion based on the different types of bridging materials that have been employed with MOFs and MOF derivatives, including graphene, CNFs, CNTs, metals, metal oxides, and conductive polymers.

Depending on their composition, these bridging materials have intrinsic advantages and disadvantages for use in materials design, suggesting the choice of supporting materials may be application-dependent. For example, all of the studied bridging materials exhibit high electronic conductivities, carbon-based supports are probably the most suitable support nanomaterials for the fabrication of flexible electrode materials, especially when compared to metals and metal oxides. Furthermore, both carbon- and metal-based bridging materials demonstrate promising conductivities and serve to generate electronic transfer pathways. Metal oxide supports generally serve as active nanomaterials, along with the introduced MOFs and MOF derivatives, which are significantly different from other composite nanomaterials where the bridging materials generally are used for bridging MOFs and MOF derivatives, attaining improved structure integrity and conductivity. Therefore, researchers should carefully consider the energy and power densities for these electrodes.

An important issue regarding electrode materials arises from the degradation of active nanomaterials during electrochemical processes, suggesting a potential disadvantage for these supported material designs. The polymers generally exhibit limited electronic conductivity, especially in comparison with metallic supports, which may potentially hamper the performance of the active nanomaterial; however, it can well-bridge the MOFs or MOF derivatives. As a potential solution, hybrid support materials that are comprised of multiple types of bridging supports may yield electrode materials with more favorable performances and greater stability. Alternatively, conductive sheets could be employed in conjunction with the bridged composite materials to yield a favorable electron transfer pathway and ionic diffusion through the complete exposure of active nanomaterials toward electrolytes, which could potentially combine multiple advantages: (i) good electronic and ionic conductivities and (ii) improved stability of the composite nanomaterial. Overall, the use of conductive bridging supports with MOFs and MOF derivatives has resulted in a promising class of nanomaterials for use in a variety of electrochemical applications, with more exciting advances surely to come.

AUTHOR INFORMATION

Corresponding Authors

Rajender S. Varma − *Regional Center of Advanced Technologies and Materials, Palacky University, Olomouc 783 71, Czech Republic;* orcid.org/0000-0001-9731-6228; Email: varma.rajender@epa.gov

Ho Won Jang − *Department of Materials Science and Engineering, Research Institute of Advanced Materials, Seoul National University, Seoul 08826, Republic of Korea;* orcid.org/0000-0002-6952-7359; Email: hwjang@snu.ac.kr

Omar K. Farha − *Department of Chemistry and International Institute of Nanotechnology, Northwestern University, Evanston, Illinois 60208, United States;* orcid.org/0000-0002-9904-9845; Email: o-farha@northwestern.edu

Mohammadreza Shokouhimehr − *Department of Materials Science and Engineering, Research Institute of Advanced Materials, Seoul National University, Seoul 08826, Republic of Korea;* orcid.org/0000-0003-1416-6805; Email: mrsh2@snu.ac.kr

Authors

Kaiqiang Zhang − *Department of Materials Science and Engineering, Research Institute of Advanced Materials, Seoul National University, Seoul 08826, Republic of Korea; Jiangsu Key Laboratory of Advanced Organic Materials, Key Laboratory of Mesoscopic Chemistry of MOE, School of Chemistry and Chemical Engineering, Nanjing University, Nanjing, Jiangsu 210023, China*

Kent O. Kirlikovali − *Department of Chemistry and International Institute of Nanotechnology, Northwestern University, Evanston, Illinois 60208, United States;* orcid.org/0000-0001-8329-1015

Quyet Van Le − *Institute of Research and Development, Duy Tan University, Da Nang 550000, Vietnam*

Zhong Jin − *Jiangsu Key Laboratory of Advanced Organic Materials, Key Laboratory of Mesoscopic Chemistry of MOE, School of Chemistry and Chemical Engineering, Nanjing University, Nanjing, Jiangsu 210023, China;* orcid.org/0000-0001-8860-8579

Complete contact information is available at: https://pubs.acs.org/10.1021/acsanm.0c00702

Notes

The authors declare no competing financial interest.

ACKNOWLEDGMENTS

This research was financially supported by the Future Material Discovery Program (2016M3D1A1027666), Basic Science Research Program (2017R1A2B3009135) through the National Research Foundation of Korea, and China Scholarship Council (201808260042). This support is appreciated. O.K.F. is grateful for the financial support from the Army Research Office (grant W911NF1910340). K.O.K. gratefully acknowledges the support from the IIN Postdoctoral Fellowship and the Northwestern University International Institute for Nanotechnology. This work was also supported by the National Key R&D Program of China (2017YFA0208200, 2016YFB0700600), the Projects of NSFC (21872069, 51761135104, 21573108), the Natural Science Foundation of Jiangsu Province (BK20180008), and the Fundamental Research Funds for the Central Universities (0205-14380188).

REFERENCES

(1) Zhang, K.; Varma, R. S.; Jang, H. W.; Choi, J.-W.; Shokouhimehr, M. Iron Hexacyanocobaltate Metal-Organic Framework: Highly Reversible and Stationary Electrode Material with Rich Borders for Lithium-Ion Batteries. *J. Alloys Compd.* **2019**, *791*, 911−917.

(2) Zhang, K.; Lee, T. H.; Jang, H. W.; Shokouhimehr, M.; Choi, J.-W. A Hybrid Energy Storage Mechanism of Zinc Hexacyanocobaltate-Based Metal-Organic Framework Endowing Stationary and High-Performance Lithium-Ion Storage. *Electron. Mater. Lett.* **2019**, *15*, 444−453.

(3) Zhang, K.; Lee, T. H.; Bubach, B.; Ostadhassan, M.; Jang, H. W.; Choi, J.-W.; Shokouhimehr, M. Layered Metal-Organic Framework

Based on Tetracyanonickelate as A Cathode Material for in situ Li-Ion Storage. *RSC Adv.* **2019**, *9*, 21363−21370.
(4) Chen, T.; Kong, W.; Zhang, Z.; Wang, L.; Hu, Y.; Zhu, G.; Chen, R.; Ma, L.; Yan, W.; Wang, Y.; Liu, J.; Jin, Z. Ionic Liquid-Immobilized Polymer Gel Electrolyte with Self-Healing Capability, High Ionic Conductivity and Heat Resistance for Dendrite-Free Lithium Metal Batteries. *Nano Energy* **2018**, *54*, 17−25.
(5) Zhang, K.; Lee, T. H.; Noh, H.; Islamoglu, T.; Farha, O. K.; Jang, H. W.; Choi, J.-W.; Shokouhimehr, M. Realization of Lithium-Ion Capacitors with Enhanced Energy Density via the Use of Gadolinium Hexacyanocobaltate as A Cathode Material. *ACS Appl. Mater. Interfaces* **2019**, *11*, 31799−31805.
(6) Zhang, K.; Lee, T. H.; Bubach, B.; Ostadhassan, M.; Jang, H. W.; Choi, J.-W.; Shokouhimehr, M. Coordinating Gallium Hexacyanocobaltate: Prussian Blue-Based Nanomaterial for Li-Ion Storage. *RSC Adv.* **2019**, *9*, 26668−26675.
(7) Wang, Y.; Xue, X.; Liu, P.; Wang, C.; Yi, X.; Hu, Y.; Ma, L.; Zhu, G.; Chen, R.; Chen, T.; Ma, J.; Liu, J.; Jin, Z. Atomic Substitution Enabled Synthesis of Vacancy-Rich Two-Dimensional Black TiO_{2-x} Nanoflakes for High-Performance Rechargeable Magnesium Batteries. *ACS Nano* **2018**, *12*, 12492−12502.
(8) Zhang, K.; Lee, T. H.; Khalilzadeh, M. A.; Varma, R. S.; Choi, J.-W.; Jang, H. W.; Shokouhimehr, M. Rendering Redox Reactions of Cathodes in Li-Ion Capacitors Enabled by Lanthanides. *ACS Omega* **2020**, *5*, 1634−1639.
(9) Zhang, K.; Lee, T. H.; Cha, J. H.; Varma, R. S.; Choi, J.-W.; Jang, H. W.; Shokouhimehr, M. Cerium Hexacyanocobaltate: A Lanthanide-Compliant Prussian Blue Analogue for Li-Ion Storage. *ACS Omega* **2019**, *4*, 21410−21416.
(10) Ma, L.; Chen, T.; Zhu, G.; Hu, Y.; Lu, H.; Chen, R.; Liang, J.; Tie, Z.; Jin, Z.; Liu, J. Pitaya-Like Microspheres Derived from Prussian Blue Analogues as Ultralong-Life Anodes for Lithium Storage. *J. Mater. Chem. A* **2016**, *4*, 15041−15048.
(11) Mehtab, T.; Yasin, G.; Arif, M.; Shakeel, M.; Korai, R. M.; Nadeem, M.; Muhammad, N.; Lu, X. Metal-Organic Frameworks for Energy Storage Devices: Batteries and Supercapacitors. *J. Energy Storage* **2019**, *21*, 632−646.
(12) Furukawa, H.; Cordova, K. E.; O'Keeffe, M.; Yaghi, O. M. The Chemistry and Applications of Metal-Organic Frameworks. *Science* **2013**, *341*, 1230444.
(13) Feng, D.; Lei, T.; Lukatskaya, M. R.; Park, J.; Huang, Z.; Lee, M.; Shaw, L.; Chen, S.; Yakovenko, A. A.; Kulkarni, A.; Xiao, J.; Fredrickson, K.; Tok, J. B.; Zou, X.; Cui, Y.; Bao, Z. Robust and Conductive Two-Dimensional Metal-Organic Frameworks with Exceptionally High Volumetric and Areal Capacitance. *Nat. Energy* **2018**, *3*, 30−36.
(14) Silva, P.; Vilela, S. M. F.; Tome, J. P. C.; Almeida Paz, F. A. Multifunctional Metal-Organic Frameworks: from Academia to Industrial Applications. *Chem. Soc. Rev.* **2015**, *44*, 6774−6803.
(15) Dang, S.; Zhu, Q.-L.; Xu, Q. Nanomaterials Derived from Metal-Organic Frameworks. *Nat. Rev. Mater.* **2018**, *3*, 17075.
(16) Khalilzadeh, M. A.; Tajik, S.; Beitollahi, H.; Venditti, R. A. Green Synthesis of Magnetic Nanocomposite with Iron Oxide Deposited on Cellulose Nanocrystals with Copper (Fe_3O_4@CNC/Cu): Investigation of Catalytic Activity for the Development of a Venlafaxine Electrochemical Sensor. *Ind. Eng. Chem. Res.* **2020**, *59*, 4219−4228.
(17) Seyednejhad, S.; Khalilzadeh, M. A.; Zareyee, D.; Sadeghifar, H.; Venditti, R. Cellulose Nanocrystal Supported Palladium as a Novel Recyclable Catalyst for Ullmann Coupling Reactions. *Cellulose* **2019**, *26*, 5015−5031.
(18) Nikahd, B.; Khalilzadeh, M. A. Liquid Phase Determination of Bisphenol A in Food Samples Using Novel Nanostructure Ionic Liquid Modified Sensor. *J. Mol. Liq.* **2016**, *215*, 253−257.
(19) Raoof, J. B.; Teymoori, N.; Khalilzadeh, M. A.; Ojani, R. A High Sensitive Electrochemical Nanosensor for Simultaneous Determination of Glutathione, NADH and Folic Acid. *Mater. Sci. Eng., C* **2015**, *47*, 77−84.
(20) Goodarzian, M.; Khalilzade, M. A.; Karimi, F.; Kumar Gupta, V.; Keyvanfard, M.; Bagheri, H.; Fouladgar, M. Square Wave Voltammetric Determination of Diclofenac in Liquid Phase Using a Novel Ionic Liquid Multiwall Carbon Nanotubes Paste Electrode. *J. Mol. Liq.* **2014**, *197*, 114−119.
(21) Khalilzadeh, M. A.; Khaleghi, F.; Gholami, F.; Karimi-Maleh, H. Electrocatalytic Determination of Ampicillin Using Carbon-Paste Electrode Modified with Ferrocendicarboxylic Acid. *Anal. Lett.* **2009**, *42*, 584−599.
(22) Khalilzadeh, M. A.; Karimi-Maleh, H.; Gupta, V. K. A Nanostructure Based Electrochemical Sensor for Square Wave Voltammetric Determination of L-Cysteine in the Presence of High Concentration of Folic Acid. *Electroanalysis* **2015**, *27*, 1766−1773.
(23) A. Khalilzadeh, M.; Arab, Z. High Sensitive Nanostructure Square Wave Voltammetric Sensor for Determination of Vanillin in Food Samples. *Curr. Anal. Chem.* **2016**, *13*, 81−86.
(24) Kharian, S.; Teymoori, N.; Khalilzadeh, M. A. Multi-Wall Carbon Nanotubes and TiO_2 as a Sensor for Electrocatalytic Determination of Epinephrinein the Presence of *p*-Chloranil as a Mediator. *J. Solid State Electrochem.* **2012**, *16*, 563−568.
(25) Raoof, J. B.; Teymoori, N.; Khalilzadeh, M. A.; Ojani, R. Synergistic Signal Amplification based on Ionic Liquid-ZnO Nanoparticle Carbon Paste Electrode for Sensitive Voltammetric Determination of Acetaminophen in the Presence of NADH. *J. Mol. Liq.* **2016**, *219*, 15−20.
(26) Popilevsky, L.; Skripnyuk, V. M.; Amouyal, Y.; Rabkin, E. Tuning the Thermal Conductivity of Hydrogenated Porous Magnesium Hydride Composites with the Aid of Carbonaceous Additives. *Int. J. Hydrogen Energy* **2017**, *42*, 22395−22405.
(27) Borisov, D. N.; Fursikov, P. V.; Tarasov, B. P. Influence of Carbonaceous Additives on Hydrogen Sorption Properties of Mg-RE-Ni "Pseudoalloys. *Int. J. Hydrogen Energy* **2011**, *36*, 1326−1329.
(28) Dungan, R. S.; Reeves, J. B. Pyrolysis of Carbonaceous Foundry Sand Additives: Seacoal and Gilsonite. *Thermochim. Acta* **2007**, *460*, 60−66.
(29) Wang, Y.; Huang, H.; Cannon, F. S.; Voigt, R. C.; Komarneni, S.; Furness, J. C. Evaluation of Volatile Hydrocarbon Emission Characteristics of Carbonaceous Additives in Green Sand Foundries. *Environ. Sci. Technol.* **2007**, *41*, 2957−2963.
(30) Taherzadeh-Ghahfarokhi, M.; Panahi, R.; Mokhtarani, B. Optimizing the Combination of Conventional Carbonaceous Additives of Culture Media to Produce Lignocellulose-Degrading Enzymes by Trichoderma Reesei in Solid State Fermentation of Agricultural Residues. *Renewable Energy* **2019**, *131*, 946−955.
(31) Apul, O. G.; Delgado, A. G.; Kidd, J.; Alam, F.; Dahlen, P.; Westerhoff, P. Carbonaceous Nano-Additives Augment Microwave-Enabled Thermal Remediation of Soils Containing Petroleum Hydrocarbons. *Environ. Sci.: Nano* **2016**, *3*, 997−1002.
(32) Kaymaksiz, S.; Kaskhedikar, N.; Sato, N.; Roth, S.; Dettlaff-Weglikowska, U. Evaluation of Synthesis Routes for Pure and Composite $LiMnPO_4$ with Carbonaceous Additives for Li-Ion Battery. In *216th ECS Meeting*, Vienna, Austria, October 4−9, 2009; The Electrochemical Society, 2009; Vol. *25*, p 187.
(33) Zhang, K.; Lee, T. H.; Bubach, B.; Jang, H. W.; Ostadhassan, M.; Choi, J.-W.; Shokouhimehr, M. Graphite Carbon-Encapsulated Metal Nanoparticles Derived from Prussian Blue Analogs Growing on Natural Loofa as Cathode Materials for Rechargeable Aluminum-Ion Batteries. *Sci. Rep.* **2019**, *9*, 13665.
(34) Zhang, K.; Lee, T. H.; Jang, H. W.; Shokouhimehr, M.; Choi, J.-W. A Hybrid Energy Storage Mechanism of Zinc Hexacyanocobaltate-Based Metal-Organic Framework Endowing Stationary and High-Performance Lithium-Ion Storage. *Electron. Mater. Lett.* **2019**, *15*, 444−453.
(35) Shokouhimehr, M.; Yu, S. H.; Lee, D. C.; Ling, D.; Hyeon, T.; Sung, Y.-E. Metal Hexacyanoferrate Nanoparticles as Electrode Materials for Lithium Ion Batteries. *Nanosci. Nanotechnol. Lett.* **2013**, *5*, 770−774.
(36) Zhang, K.; Lee, T. H.; Cha, J. H.; Jang, H. W.; Choi, J.-W.; Mahmoudi, M.; Shokouhimehr, M. Metal-Organic Framework-

https://dx.doi.org/10.1021/acsanm.0c00702
ACS Appl. Nano Mater. 2020, 3, 3964−3990

Derived Metal Oxide Nanoparticles@Reduced Graphene Oxide Composites as Cathode Materials for Rechargeable Aluminium-Ion Batteries. *Sci. Rep.* **2019**, *9*, 13739.
(37) Xie, Z.; Xu, W.; Cui, X.; Wang, Y. Recent Progress in Metal-Organic Frameworks and Their Derived Nanostructures for Energy and Environmental Applications. *ChemSusChem* **2017**, *10*, 1645–1663.
(38) Yu, S. H.; Shokouhimehr, M.; Hyeon, T.; Sung, Y.-E. Iron Hexacyanoferrate Nanoparticles as Cathode Materials for Lithium and Sodium Rechargeable Batteries. *ECS Electrochem. Lett.* **2013**, *2*, A39–A41.
(39) Dang, S.; Zhu, Q. L.; Xu, Q. Nanomaterials Derived from Metal-Organic Frameworks. *Nat. Rev. Mater.* **2018**, *3*, 17075.
(40) Wang, L.; Han, Y.; Feng, X.; Zhou, J.; Qi, P.; Wang, B. Metal-Organic Frameworks for Energy Storage: Batteries and Supercapacitors. *Coord. Chem. Rev.* **2016**, *307*, 361–381.
(41) Zhang, H.; Nai, J.; Yu, L.; Lou, X. W. Metal-Organic-Framework-Based Materials as Platforms for Renewable Energy and Environmental Applications. *Joule* **2017**, *1*, 77–107.
(42) Wu, H. B.; Lou, X. W. Metal-Organic Frameworks and Their Derived Materials for Electrochemical Energy Storage and Conversion: Promises and Challenges. *Sci. Adv.* **2017**, *3*, eaap9252.
(43) Yang, W.; Li, X.; Li, Y.; Zhu, R.; Pang, H. Applications of Metal-Organic-Framework-Derived Carbon Materials. *Adv. Mater.* **2018**, *31*, 1804740.
(44) Guan, B. Y.; Yu, X. Y.; Wu, H. B.; Lou, X. W. Complex Nanostructures from Materials Based on Metal-Organic Frameworks for Electrochemical Energy Storage and Conversion. *Adv. Mater.* **2017**, *29*, 1703614.
(45) Cao, X.; Tan, C.; Sindoro, M.; Zhang, H. Hybrid Micro-/Nano-Structures Derived from Metal-Organic Frameworks: Preparation and Applications in Energy Storage and Conversion. *Chem. Soc. Rev.* **2017**, *46*, 2660–2677.
(46) Fu, Y.; Hu, J.; Wang, Q.; Lin, D.; Li, K.; Zhou, L. Thermally Etched Porous Carbon Cloth Catalyzed by Metal Organic Frameworks as Sulfur Hosts for Lithium-Sulfur Batteries. *Carbon* **2019**, *150*, 76–84.
(47) Zhang, L.; Zhang, Y.; Huang, S.; Yuan, Y.; Li, H.; Jin, Z.; Wu, J.; Liao, Q.; Hu, L.; Lu, J.; Ruan, S.; Zeng, Y.-J. Co_3O_4/Ni-Based MOFs on Carbon Cloth for Flexible Alkaline Battery-Supercapacitor Hybrid Devices and Near-Infrared Photocatalytic Hydrogen Evolution. *Electrochim. Acta* **2018**, *281*, 189–197.
(48) Rawool, C. R.; Karna, S. P.; Srivastava, A. K. Enhancing the Supercapacitive Performance of Nickel Based Metal Organic Framework-Carbon Nanofibers Composite by Changing the Ligands. *Electrochim. Acta* **2019**, *294*, 345–356.
(49) Liu, X.; Guan, C.; Hu, Y.; Zhang, L.; Elshahawy, A. M.; Wang, J. 2D Metal-Organic Frameworks Derived Nanocarbon Arrays for Substrate Enhancement in Flexible Supercapacitors. *Small* **2018**, *14*, 1702641.
(50) Li, X.; Wu, H.; Elshahawy, A. M.; Wang, L.; Pennycook, S. J.; Guan, C.; Wang, J. Cactus-Like NiCoP/NiCo-OH 3D Architecture with Tunable Composition for High-Performance Electrochemical Capacitors. *Adv. Funct. Mater.* **2018**, *28*, 1800036.
(51) Guan, C.; Zhao, W.; Hu, Y.; Lai, Z.; Li, X.; Sun, S.; Zhang, H.; Cheetham, A. K.; Wang, J. Cobalt Oxide and N-doped Carbon Nanosheets Derived from A Single Two-Dimensional Metal-Organic Framework Precursor and Their Application in Flexible Asymmetric Supercapacitors. *Nanoscale Horiz.* **2017**, *2*, 99–105.
(52) Qi, K.; Hou, R.; Zaman, S.; Qiu, Y.; Xia, B. Y.; Duan, H. Construction of Metal-Organic Framework/Conductive Polymer Hybrid for All-Solid-State Fabric Supercapacitor. *ACS Appl. Mater. Interfaces* **2018**, *10*, 18021–18028.
(53) Zhao, S.; Wu, H.; Li, Y. L.; Li, Q.; Zhou, J.; Yu, X.; Chen, H.; Tao, K.; Han, L. Core-Shell Assembly of Carbon Nanofiber and 2D Conductive Metal-Organic Framework as Flexible Free-Standing Membrane for High-Performance Supercapacitor. *Inorg. Chem. Front.* **2019**, *6*, 1824–1830.
(54) Young, C.; Wang, J.; Kim, J.; Sugahara, Y.; Henzie, J.; Yamauchi, Y. Controlled Chemical Vapor Deposition for Synthesis of Nanowire Arrays of Metal-Organic Frameworks and Their Thermal Conversion to Carbon/Metal Oxide Hybrid Materials. *Chem. Mater.* **2018**, *30*, 3379–3386.
(55) Srimuk, P.; Luanwuthi, S.; Krittayavathananon, A.; Sawangphruk, M. Solid-Type Supercapacitor of Reduced Graphene Oxide-Metal Organic Framework Composite Coated on Carbon Fiber Paper. *Electrochim. Acta* **2015**, *157*, 69–77.
(56) Liu, Y.; Ma, J.; Lu, T.; Pan, L. Electrospun Carbon Nanofibers Reinforced 3D Porous Carbon Polyhedra Network Derived from Metal-Organic Frameworks for Capacitive Deionization. *Sci. Rep.* **2016**, *6*, 32784.
(57) Xu, D.; Chao, D.; Wang, H.; Gong, Y.; Wang, R.; He, B.; Hu, X.; Fan, J. H. Flexible Quasi-Solid-State Sodium-Ion Capacitors Developed Using 2D Metal-Organic-Framework Array as Reactor. *Adv. Energy Mater.* **2018**, *8*, 1702769.
(58) Wang, L.; Feng, X.; Ren, L.; Piao, Q.; Zhong, J.; Wang, Y.; Li, H.; Chen, Y.; Wang, B. Flexible Solid-State Supercapacitor Based on A Metal-Organic Framework Interwoven by Electrochemically-Deposited PANI. *J. Am. Chem. Soc.* **2015**, *137*, 4920–4923.
(59) Guan, C.; Liu, X.; Ren, W.; Li, X.; Cheng, C.; Wang, J. Rational Design of Metal-Organic Framework Derived Hollow $NiCo_2O_4$ Arrays for Flexible Supercapacitor and Electrocatalysis. *Adv. Energy Mater.* **2017**, *7*, 1602391.
(60) Ke, Q.; Guan, C.; Zhang, X.; Zheng, M.; Zhang, Y.-W.; Cai, Y.; Zhang, H.; Wang, J. Surface-Charge-Mediated Formation of H-TiO_2@$Ni(OH)_2$ Heterostructures for High-Performance Supercapacitors. *Adv. Mater.* **2017**, *29*, 1604164.
(61) Zhang, Y.; Su, Q.; Xu, W.; Cao, G.; Wang, Y.; Pan, A.; Liang, S. A Confined Replacement Synthesis of Bismuth Nanodots in MOF Derived Carbon Arrays as Binder-Free Anodes for Sodium-Ion Batteries. *Adv. Sci.* **2019**, *6*, 1900162.
(62) Li, C.; Zhang, Q.; Sun, J.; Li, T.; E, S.; Zhu, Z.; He, B.; Zhou, Z.; Li, Q.; Yao, Y. High-Performance Quasi-Solid-State Flexible Aqueous Rechargeable Ag-Zn Battery Based on Metal-Organic Framework-Derived Ag Nanowires. *ACS Energy Lett.* **2018**, *3*, 2761–2768.
(63) Guan, C.; Sumboja, A.; Wu, H.; Ren, W.; Liu, X.; Zhang, H.; Liu, Z.; Cheng, C.; Pennycook, S. J.; Wang, J. Hollow Co_3O_4 Nanosphere Embedded in Carbon Arrays for Stable and Flexible Solid-State Zinc-Air Batteries. *Adv. Mater.* **2017**, *29*, 1704117.
(64) Li, J.; Zhao, H.; Wang, J.; Li, N.; Wu, M.; Zhang, Q.; Du, Y. Interplanar Space-Controllable Carboxylate Pillared Metal Organic Framework Ultrathin Nanosheet for Superhigh Capacity Rechargeable Alkaline Battery. *Nano Energy* **2019**, *62*, 876–882.
(65) Chen, T.; Li, S.; Wen, J.; Gui, P.; Fang, G. Metal-Organic Framework Template Derived Porous $CoSe_2$ Nanosheet Arrays for Energy Conversion and Storage. *ACS Appl. Mater. Interfaces* **2017**, *9*, 35927–35935.
(66) Zeng, W.; Wang, L.; Shi, H.; Zhang, G.; Zhang, K.; Zhang, H.; Gong, F.; Wang, T.; Duan, H. Metal-Organic-Framework-Derived ZnO@C@$NiCo_2O_4$ Core-Shell Structures as an Advanced Electrode for High-Performance Supercapacitors. *J. Mater. Chem. A* **2016**, *4*, 8233–8241.
(67) Zhang, W.; Yue, Z.; Wang, Q.; Zeng, X.; Fu, C.; Li, Q.; Li, X.; Fang, L.; Li, L. Carbon-Encapsulated CoS_2 Nanoparticles Anchored on N-Doped Carbon Nanofibers Derived from ZIF-8/ZIF-67 as Anode for Sodium-Ion Batteries. *Chem. Eng. J.* **2020**, *380*, 122548.
(68) Ren, W.; Zhang, H.; Guan, C.; Cheng, C. Ultrathin MoS_2 Nanosheets@Metal Organic Framework-Derived n-Doped Carbon Nanowall Arrays as Sodium Ion Battery Anode with Superior Cycling Life and Rate Capability. *Adv. Funct. Mater.* **2017**, *27*, 1702116.
(69) Yu, H.; Zhu, W.; Zhou, H.; Liu, J.; Yang, Z.; Hu, X.; Yuan, A. Porous Carbon Derived from Metal-Organic Framework@Graphene Quantum Dots as Electrode Materials for Supercapacitors and Lithium-Ion Batteries. *RSC Adv.* **2019**, *9*, 9577–9583.

https://dx.doi.org/10.1021/acsanm.0c00702
ACS Appl. Nano Mater. 2020, 3, 3964–3990

(70) Xu, Y.; Hou, S.; Yang, G.; Lu, T.; Pan, L. NiO/CNTs Derived from Metal-Organic Frameworks as Superior Anode Material for Lithium-Ion Batteries. *J. Solid State Electrochem.* **2018**, *22*, 785−795.
(71) Tan, B.; Wu, Z. F.; Xie, Z. L. Fine Decoration of Carbon Nanotubes with Metal Organic Frameworks for Enhanced Performance in Supercapacitance and Oxygen Reduction Reaction. *Sci. Bull.* **2017**, *62*, 1132−1141.
(72) Xu, C.; Kong, X.; Zhou, S.; Zheng, B.; Huo, F.; Strømme, M. Interweaving Metal-Organic Framework-Templated Co-Ni Layered Double Hydroxide Nanocages with Nanocellulose and Carbon Nanotubes to Make Flexible and Foldable Electrodes for Energy Storage Devices. *J. Mater. Chem. A* **2018**, *6*, 24050−24057.
(73) Tang, Q.; Wang, W.; Wang, G. The Perfect Matching between the Low-Cost Fe_2O_3 Nanowire Anode and the NiO Nanoflake Cathode Significantly Enhances the Energy Density of Asymmetric Supercapacitors. *J. Mater. Chem. A* **2015**, *3*, 6662−6670.
(74) Liu, Z.; Tian, X.; Xu, X.; He, L.; Yan, M.; Han, C.; Li, Y.; Yang, W.; Mai, L. Capacitance and Voltage Matching between MnO_2 Nanoflake Cathode and Fe_2O_3 Nanoparticle Anode for High-Performance Asymmetric Micro-Supercapacitors. *Nano Res.* **2017**, *10*, 2471−2481.
(75) Yang, C.; Sun, M.; Wang, G.; Cheng, Q.; Bao, H.; Li, X.; Saha, N.; Saha, P. High Energy-Density Organic Supercapacitors based on Optimum Matching between GNS/aMWCNT@Polyaniline Nanocone Arrays Cathode and GNS/aMWCNT@poly (1,5-Diaminoanthraquinone) Nanoparticles Anode. *Chem. Eng. J.* **2017**, *326*, 9−16.
(76) Yang, S. H.; Park, S. K.; Kang, Y. C. Mesoporous $CoSe_2$ Nanoclusters Threaded with Nitrogen-Doped Carbon Nanotubes for High-Performance Sodium-Ion Battery Anodes. *Chem. Eng. J.* **2019**, *370*, 1008−1018.
(77) Huang, G.; Zhang, F.; Du, X.; Qin, Y.; Yin, D.; Wang, L. Metal Organic Frameworks Route to in Situ Insertion of Multiwalled Carbon Nanotubes in Co_3O_4 Polyhedra as Anode Materials for Lithium-Ion Batteries. *ACS Nano* **2015**, *9*, 1592−1599.
(78) Zhou, Z.; Zhang, Q.; Sun, J.; He, B.; Guo, J.; Li, Q.; Li, C.; Xie, L.; Yao, Y. Metal-Organic Framework Derived Spindle-Like Carbon Incorporated α-Fe_2O_3 Grown on Carbon Nanotube Fiber as Anodes for High-Performance Wearable Asymmetric Supercapacitors. *ACS Nano* **2018**, *12*, 9333−9341.
(79) Jiao, G.; Gu, Y.; Wang, J.; Wu, D.; Tao, S.; Chu, S.; Liu, Y.; Qian, B.; Chu, W. Porous CoP/C@MCNTs Hybrid Composite Derived from Metal-Organic Frameworks for High-Performance Lithium-Ion Batteries. *J. Mater. Sci.* **2019**, *54*, 3273−3283.
(80) He, B.; Zhang, Q.; Man, P.; Zhou, Z.; Li, C.; Li, Q.; Xie, L.; Wang, X.; Pang, H.; Yao, Y. Self-Sacrificed Synthesis of Conductive Vanadium-Based Metal-Organic Framework Nanowire-Bundle Arrays as Binder-Free Cathodes for High-Rate and High-Energy-Density Wearable Zn-Ion Batteries. *Nano Energy* **2019**, *64*, 103935.
(81) Tang, X.; Liang, M.; Zhang, Y.; Sun, W.; Wang, Y. Ultrafine Ternary Metal Oxide Particles with Carbon Nanotubes: a Metal-Organic-Framework-Based Approach and Superior Lithium-Storage Performance. *Dalton T.* **2019**, *48*, 4413−4419.
(82) Tabassum, H.; Guo, W.; Meng, W.; Mahmood, A.; Zhao, R.; Wang, Q.; Zou, R. Metal-Organic Frameworks Derived Cobalt Phosphide Architecture Encapsulated into B/N Co-Doped Graphene Nanotubes for All pH Value Electrochemical Hydrogen Evolution. *Adv. Energy Mater.* **2017**, *7*, 1601671.
(83) Gao, T.; Zhou, F.; Ma, W.; Li, H. Metal-Organic-Framework Derived Carbon Polyhedron and Carbon Nanotube Hybrids as Electrode for Electrochemical Supercapacitor and Capacitive Deionization. *Electrochim. Acta* **2018**, *263*, 85−93.
(84) Xiong, P.; Zhao, X.; Xu, Y. Nitrogen-Doped Carbon Nanotubes Derived from Metal−Organic Frameworks for Potassium-Ion Battery Anodes. *ChemSusChem* **2018**, *11*, 202−208.
(85) Lei, K.; Ling, J.; Zhou, J.; Zou, H.; Yang, W.; Chen, S. Formation of CoS_2/N, S-co-Doped Porous Carbon Nanotube Composites Based on Bimetallic Zeolitic Imidazolate Organic Frameworks for Supercapacitors. *Mater. Res. Bull.* **2019**, *116*, 59−66.
(86) Wang, P.; Li, C.; Wang, W.; Wang, J.; Zhu, Y.; Wu, Y. Hollow Co_9S_8 from Metal Organic Framework Supported on rGO as Electrode Material for Highly Stable Supercapacitors. *Chin. Chem. Lett.* **2018**, *29*, 612−615.
(87) Jayakumar, A.; Antony, R. P.; Wang, R.; Lee, J.-M. MOF-Derived Hollow Cage $Ni_xCo_{3-x}O_4$ and Their Synergy with Graphene for Outstanding Supercapacitors. *Small* **2017**, *13*, 1603102.
(88) Wang, S.; Ning, P.; Huang, S.; Wang, W.; Fei, S.; He, Q.; Zai, J.; Jiang, Y.; Hu, Z.; Qian, X.; Chen, Z. Multi-Functional NiS_2/FeS_2/N-Doped Carbon Nanorods Derived from Metal-Organic Frameworks with Fast Reaction Kinetics for High Performance Overall Water Splitting and Lithium-Ion Batteries. *J. Power Sources* **2019**, *436*, 226857.
(89) Huang, J.; Tang, X.; Li, Z.; Liu, K. Metal Organic Frameworks Derived Cobalt Sulfide/Reduced Graphene Oxide Composites with Fast Reaction Kinetic and Excellent Structural Stability for Sodium Storage. *J. Colloid Interface Sci.* **2018**, *532*, 407−415.
(90) Niu, J. L.; Peng, H. J.; Zeng, C. H.; Lin, X.-M.; Sathishkumar, P.; Cai, Y.-P.; Xu, A.-W. An Efficient Multidoped $Cu_{0.39}Zn_{0.14}Co_{2.47}O_4$-ZnO Electrode Attached on Reduced Graphene Oxide and Copper Foam as Superior Lithium-Ion Battery Anodes. *Chem. Eng. J.* **2018**, *336*, 510−517.
(91) Zhang, W.; Tan, Y.; Gao, Y.; Wu, J.; Hu, J.; Stein, A.; Tang, B. Nanocomposites of Zeolitic Imidazolate Frameworks on Graphene Oxide for Pseudocapacitor Applications. *J. Appl. Electrochem.* **2016**, *46*, 441−450.
(92) Chen, S.; Cai, D.; Yang, X.; Chen, Q.; Zhan, H.; Qu, B.; Wang, T. Metal-Organic Frameworks Derived Nanocomposites of Mixed-Valent MnO_x Nanoparticles In-Situ Grown on Ultrathin Carbon Sheets for High-Performance Supercapacitors and Lithium-Ion Batteries. *Electrochim. Acta* **2017**, *256*, 63−72.
(93) Tabassum, H.; Mahmood, A.; Wang, Q.; Xia, W.; Liang, Z.; Qiu, B.; Zhao, R.; Zou, R. Hierarchical Cobalt Hydroxide and B/N co-Doped Graphene Nanohybrids Derived from Metal-Organic Frameworks for High Energy Density Asymmetric Supercapacitors. *Sci. Rep.* **2017**, *7*, 43084.
(94) Islam, D. A.; Chakraborty, A.; Roy, A.; Das, S.; Acharya, H. Fabrication of Graphene-Oxide (GO)-Supported Sheet-Like CuO Nanostructures Derived from a Metal-Organic-Framework Template for High-Performance Hybrid Supercapacitors. *ChemistrySelect* **2018**, *3*, 11816−11823.
(95) Zhao, K.; Lyu, K.; Liu, S.; Gan, Q.; He, Z.; Zhou, Z. Ordered Porous Mn_3O_4@N-Doped Carbon/Graphene Hybrids Derived from Metal-Organic Frameworks for Supercapacitor Electrodes. *J. Mater. Sci.* **2017**, *52*, 446−457.
(96) Tan, L.; Guo, D.; Liu, J.; Song, X.; Liu, Q.; Chen, R.; Wang, J. In-Situ Calcination of Polyoxometallate-Based Metal Organic Framework/Reduced Graphene Oxide Composites Towards Supercapacitor Electrode with Enhanced Performance. *J. Electroanal. Chem.* **2019**, *836*, 112−117.
(97) Ma, L.; Fan, H.; Fu, K.; Zhao, Y. Metal-Organic Framework/Layered Carbon Nitride Nano-sandwiches for Superior Asymmetric Supercapacitor. *ChemistrySelect* **2016**, *1*, 3730−3738.
(98) Punde, N. S.; Rawool, C. R.; Rajpurohit, A. S.; Karna, S. P.; Srivastava, A. K. Hybrid Composite Based on Porous Cobalt-Benzenetricarboxylic Acid Metal Organic Framework and Graphene Nanosheets as High Performance Supercapacitor Electrode. *ChemistrySelect* **2018**, *3*, 11368−11380.
(99) Azadfalah, M.; Sedghi, A.; Hosseini, H. Synthesis of Nano-Flower Metal-Organic Framework/Graphene Composites as a High-Performance Electrode Material for Supercapacitors. *J. Electron. Mater.* **2019**, *48*, 7011−7024.
(100) Xin, L.; Liu, Q.; Liu, J.; Chen, R.; Li, R.; Li, Z.; Wang, J. Hierarchical Metal-Organic Framework Derived Nitrogen-Doped Porous Carbon/Graphene Composite for High Performance Supercapacitors. *Electrochim. Acta* **2017**, *248*, 215−224.
(101) Azadfalah, M.; Sedghi, A.; Hosseini, H. Synergistic Effect of Ni-Based Metal Organic Framework with Graphene for Enhanced

https://dx.doi.org/10.1021/acsanm.0c00702
ACS Appl. Nano Mater. 2020, 3, 3964−3990

Electrochemical Performance of Supercapacitors. *J. Mater. Sci.: Mater. Electron.* **2019**, *30*, 12351−12363.
(102) Hong, J.; Park, S. J.; Kim, S. Synthesis and Electrochemical Characterization of Nanostructured Ni-Co-MOF/Graphene Oxide Composites as Capacitor Electrodes. *Electrochim. Acta* **2019**, *311*, 62−71.
(103) Rajpurohit, A. S.; Punde, N. S.; Srivastava, A. K. A Dual Metal Organic Framework Based on Copper-Iron Clusters Integrated Sulphur Doped Graphene as A Porous Material for Supercapacitor with Remarkable Performance Characteristics. *J. Colloid Interface Sci.* **2019**, *553*, 328−340.
(104) Rahmanifar, M. S.; Hesari, H.; Noori, A.; Masoomi, M. Y.; Morsali, A.; Mousavi, M. F. A Dual Ni/Co-MOF-Reduced Graphene Oxide Nanocomposite as A High Performance Supercapacitor Electrode Material. *Electrochim. Acta* **2018**, *275*, 76−86.
(105) Jiao, Y.; Pei, J.; Chen, D.; Yan, C.; Hu, Y.; Zhang, Q.; Chen, G. Mixed-Metallic MOF Based Electrode Materials for High Performance Hybrid Supercapacitors. *J. Mater. Chem. A* **2017**, *5*, 1094−1102.
(106) Chen, C.; Wu, M.; Tao, K.; Zhou, J.; Li, Y.; Han, X.; Han, L. Formation of Bimetallic Metal-Organic Frameworks Nanosheets and Their Derived Porous Nickel-Cobalt Sulfides for Supercapacitors. *Dalton T.* **2018**, *47*, 5639−5645.
(107) Kazemi, S.; Hosseinzadeh, B.; Kazemi, H.; Kiani, M.; Hajati, S. Applications Facile Synthesis of Mixed Metal Organic Frameworks: Electrode Materials for Supercapacitor with Excellent Areal Capacitance and Operational Stability. *ACS Appl. Mater. Interfaces* **2018**, *10*, 23063−23073.
(108) Yu, D.; Ge, L.; Wei, X.; Wu, B.; Ran, J.; Wang, H.; Xu, T. A General Route to the Synthesis of Layer-by-Layer Structured Metal Organic Framework/Graphene Oxide Hybrid Films for High-Performance Supercapacitor Electrodes. *J. Mater. Chem. A* **2017**, *5*, 16865−16872.
(109) Zhou, Y.; Mao, Z.; Wang, W.; Yang, Z.; Liu, X. In-Situ Fabrication of Graphene Oxide Hybrid Ni-Based Metal-Organic Framework (Ni-MOFs@GO) with Ultrahigh Capacitance as Electrochemical Pseudocapacitor Materials. *ACS Appl. Mater. Interfaces* **2016**, *8*, 28904−28916.
(110) Zheng, X.; Cao, Y.; Liu, D.; Cai, M.; Ding, J.; Liu, X.; Wang, J.; Hu, W.; Zhong, C. Bimetallic Metal-Organic-Framework/Reduced Graphene Oxide Composites as Bifunctional Electrocatalysts for Rechargeable Zn-Air Batteries. *ACS Appl. Mater. Interfaces* **2019**, *11*, 15662−15669.
(111) Wang, L.; Wei, T.; Sheng, L.; Jiang, L.; Wu, X.; Zhou, Q.; Yuan, B.; Yue, J.; Liu, Z.; Fan, Z. Brick-and-Mortar" Sandwiched Porous Carbon Building Constructed by Metal-Organic Framework and Graphene: Ultrafast Charge/Discharge Rate Up to 2 V s^{-1} for Supercapacitors. *Nano Energy* **2016**, *30*, 84−92.
(112) Bai, X.; Liu, Q.; Lu, Z.; Liu, J.; Chen, R.; Li, R.; Song, D.; Jing, X.; Liu, P.; Wang, J. Rational Design of Sandwiched Ni-Co Layered Double Hydroxides Hollow Nanocages/Graphene Derived from Metal-Organic Framework for Sustainable Energy Storage. *ACS Sustainable Chem. Eng.* **2017**, *5*, 9923−9934.
(113) Wei, T.; Zhang, M.; Wu, P.; Tang, Y.-J.; Li, S.-L.; Shen, F.-C.; Wang, X.-L.; Zhou, X.-P.; Lan, Y.-Q. POM-Based Metal-Organic Framework/Reduced Graphene Oxide Nanocomposites with Hybrid Behavior of Battery-Supercapacitor for Superior Lithium Storage. *Nano Energy* **2017**, *34*, 205−214.
(114) Xie, J.; Zhu, Y.; Zhuang, N.; Lei, H.; Zhu, W.; Fu, Y.; Javed, M. S.; Li, J.; Mai, W. Rational Design of Metal Organic Framework-Derived FeS_2 Hollow Nanocages@Reduced Graphene Oxide for K-Ion Storage. *Nanoscale* **2018**, *10*, 17092−17098.
(115) Banerjee, P. C.; Lobo, D. E.; Middag, R.; Ng, W. K.; Shaibani, M. E.; Majumder, M. Electrochemical Capacitance of Ni-Doped Metal Organic Framework and Reduced Graphene Oxide Composites: More Than the Sum of Its Parts. *ACS Appl. Mater. Interfaces* **2015**, *7*, 3655−3664.
(116) Xu, X.; Shi, W.; Li, P.; Ye, S.; Ye, C.; Ye, H.; Lu, T.; Zheng, A.; Zhu, J.; Xu, L.; Zhong, M.; Cao, X. Facile Fabrication of Three-Dimensional Graphene and Metal-Organic Framework Composites and Their Derivatives for Flexible All-Solid-State Supercapacitors. *Chem. Mater.* **2017**, *29*, 6058−6065.
(117) Xia, W.; Qu, C.; Liang, Z.; Zhao, B.; Dai, S.; Qiu, B.; Jiao, Y.; Zhang, Q.; Huang, X.; Guo, W.; Dang, D.; Zou, R.; Xia, D.; Xu, Q.; Liu, M. High-Performance Energy Storage and Conversion Materials Derived from A Single Metal-Organic Framework/Graphene Aerogel Composite. *Nano Lett.* **2017**, *17*, 2788−2795.
(118) Shuang, W.; Huang, H.; Kong, L.; Zhong, M.; Li, A.; Wang, D.; Xu, Y.; Bu, X.-H. Nitrogen-Doped Carbon Shell-Confined Ni_3S_2 Composite Nanosheets Derived from Ni-MOF for High Performance Sodium-Ion Battery Anodes. *Nano Energy* **2019**, *62*, 154−163.
(119) Pilban Jahromi, S.; Pandikumar, A.; Goh, B. T.; Lim, Y. S.; Basirun, W. J.; Lim, H. N.; Huang, N. M. Influence of particle size on performance of a nickel oxide nanoparticle-based supercapacitor. *RSC Adv.* **2015**, *5*, 14010−14019.
(120) Liu, H.; Wang, J.; Zhang, X.; Zhou, D.; Qi, X.; Qiu, B.; Fang, J.; Kloepsch, R.; Schumacher, G.; Liu, Z.; Li, J. Morphological evolution of high-voltage spinel $LiNi_{0.5}Mn_{1.5}O_4$ cathode materials for lithium-ion batteries: the critical effects of surface orientations and particle size. *ACS Appl. Mater. ACS Appl. Mater. Interfaces* **2016**, *8* (7), 4661−4675.
(121) Duraisamy, N.; Numan, A.; Fatin, S. O.; Ramesh, K.; Ramesh, S. Facile sonochemical synthesis of nanostructured NiO with different particle sizes and its electrochemical properties for supercapacitor application. *J. Colloid Interface Sci.* **2016**, *471*, 136−144.
(122) Xiao, P.; Bu, F.; Zhao, R.; Aly Aboud, M. F.; Shakir, I.; Xu, Y. Sub-5 nm Ultrasmall Metal-Organic Framework Nanocrystals for Highly Efficient Electrochemical Energy Storage. *ACS Nano* **2018**, *12*, 3947−3953.
(123) Cao, X.; Zheng, B.; Shi, W.; Yang, J.; Fan, Z.; Luo, Z.; Rui, X.; Chen, B.; Yan, Q.; Zhang, H. Reduced Graphene Oxide-Wrapped MoO_3 Composites Prepared by Using Metal-Organic Frameworks as Precursor for All-Solid-State Flexible Supercapacitors. *Adv. Mater.* **2015**, *27*, 4695−4701.
(124) Cheng, J.; Chen, S.; Chen, D.; Dong, L.; Wang, J.; Zhang, T.; Jiao, T.; Liu, B.; Wang, H.; Kai, J.-J.; Zhang, D.; Zheng, G.; Zhi, L.; Kang, F.; Zhang, W. Editable Asymmetric All-Solid-State Supercapacitors Based on High-Strength, Flexible, and Programmable 2D-Metal-Organic Framework/Reduced Graphene Oxide Self-Assembled Papers. *J. Mater. Chem. A* **2018**, *6*, 20254−20266.
(125) Zhao, G.; Liu, Y.; Tang, L.; Zhang, L.; Sun, K. Capacitive Behavior Based on the Ultrafast Mass Transport in a Self-Supported Lithium Oxygen Battery Cathode. *ACS Appl. Energy Mater.* **2019**, *2*, 2113−2121.
(126) Xu, X.; Liu, Z.; Ji, S.; Wang, Z.; Ni, Z.; Lv, Y.; Liu, J.; Liu, J. Rational Synthesis of Ternary FeS@TiO_2@C Nanotubes as Anode for Superior Na-Ion Batteries. *Chem. Eng. J.* **2019**, *359*, 765−774.
(127) Li, Y. L.; Zhou, J. J.; Wu, M. K.; Chen, C.; Tao, K.; Yi, F.-Y.; Han, L. Hierarchical Two-Dimensional Conductive Metal-Organic Framework/Layered Double Hydroxide Nanoarray for A High-Performance Supercapacitor. *Inorg. Chem.* **2018**, *57*, 6202−6205.
(128) Mohd Zain, N. K.; Vijayan, B. L.; Misnon, I. I.; Das, S.; Karuppiah, C.; Yang, C.-C.; Yusoff, M. M.; Jose, R. Direct Growth of Triple Cation Metal-Organic Framework on a Metal Substrate for Electrochemical Energy Storage. *Ind. Eng. Chem. Res.* **2019**, *58*, 665−674.
(129) Yang, J.; Zeng, C.; Wei, F.; Jiang, J.; Chen, K.; Lu, S. Cobalt-Carbon Derived from Zeolitic Imidazolate Framework on Ni Foam as High-Performance Supercapacitor Electrode Material. *Mater. Des.* **2015**, *83*, 552−556.
(130) Fan, X.; Chen, W.; Pang, S.; Lu, W.; Zhao, Y.; Liu, Z.; Fang, D. Asymmetric Supercapacitors Utilizing Highly Porous Metal-Organic Framework Derived Co_3O_4 Nanosheets Grown on Ni Foam and Polyaniline Hydrogel Derived N-Doped Nanocarbon Electrode Materials. *Chem. Phys. Lett.* **2017**, *689*, 162−168.
(131) Wang, J.; Zhong, Q.; Zeng, Y.; Cheng, D.; Xiong, Y.; Bu, Y. Rational Construction of Triangle-like Nickel-Cobalt Bimetallic Metal-Organic Framework Nanosheets Arrays as Battery-Type

https://dx.doi.org/10.1021/acsanm.0c00702
ACS Appl. Nano Mater. 2020, 3, 3964−3990

Electrodes for Hybrid Supercapacitors. *J. Colloid Interface Sci.* **2019**, *555*, 42−52.
(132) Bahaa, A.; Balamurugan, J.; Kim, N. H.; Lee, J. H. Metal-Organic Framework Derived Hierarchical Copper Cobalt Sulfide Nanosheet Arrays for High-Performance Solid-State Asymmetric Supercapacitors. *J. Mater. Chem. A* **2019**, *7*, 8620−8632.
(133) Guo, D.; Song, X.; Tan, L.; Ma, H.; Pang, H.; Wang, X.; Zhang, L. Metal-Organic Framework Template-Directed Fabrication of Well-Aligned Pentagon-like Hollow Transition-Metal Sulfides as the Anode and Cathode for High-Performance Asymmetric Supercapacitors. *ACS Appl. Mater. Interfaces* **2018**, *10*, 42621−42629.
(134) Ren, J. T.; Yuan, G. G.; Weng, C. C.; Yuan, Z.-Y. Rationally Designed Co_3O_4-C Nanowire Arrays on Ni Foam Derived from Metal Organic Framework as Reversible Oxygen Evolution Electrodes with Enhanced Performance for Zn-Air Batteries. *ACS Sustainable Chem. Eng.* **2018**, *6*, 707−718.
(135) Li, Q.; Li, Y.; Zhao, J.; Zhao, S.; Zhou, J.; Chen, C.; Tao, K.; Liu, R.; Han, L. Ultrathin Nanosheet-Assembled Hollow Microplate $CoMoO_4$ Array Derived from Metal-Organic Framework for Supercapacitor with Ultrahigh Areal Capacitance. *J. Power Sources* **2019**, *430*, 51−59.
(136) Zhao, G.; Sun, X.; Zhang, L.; Chen, X.; Mao, Y.; Sun, K. A Self-Supported Metal-Organic Framework Derived Co_3O_4 Film Prepared by an In-Situ Electrochemically Assistant Process as Li Ion Battery Anodes. *J. Power Sources* **2018**, *389*, 8−12.
(137) Hong, M.; Zhou, C.; Xu, S.; Ye, X.; Yang, Z.; Zhang, L.; Zhou, Z.; Hu, N.; Zhang, Y. Bi-Metal Organic Framework Nanosheets Assembled on Nickel Wire Films for Volumetric-Energy-Dense Supercapacitors. *J. Power Sources* **2019**, *423*, 80−89.
(138) Cheng, C. F.; Li, X.; Liu, K.; Zou, F.; Tung, W.-Y.; Huang, Y.-F.; Xia, X.; Wang, C.-L.; Vogt, B. D.; Zhu, Y. A High-Performance Lithium-Ion Capacitor with Carbonized $NiCo_2O_4$ Anode and Vertically-Aligned Carbon Nanoflakes Cathode. *Energy Storage Mater.* **2019**, *22*, 265−274.
(139) Chen, H.; Wang, M. Q.; Yu, Y.; Liu, H.; Lu, S.-Y.; Bao, S.-J.; Xu, M. Assembling Hollow Cobalt Sulfide Nanocages Array on Graphene-like Manganese Dioxide Nanosheets for Superior Electrochemical Capacitors. *ACS Appl. Mater. Interfaces* **2017**, *9*, 35040−35047.
(140) Li, H.; Yu, M.; Wang, F.; Liu, P.; Liang, Y.; Xiao, J.; Wang, C.; Tong, Y.; Yang, G. Amorphous Nickel Hydroxide Nanospheres with Ultrahigh Capacitance and Energy Density as Electrochemical Pseudocapacitor Materials. *Nat. Commun.* **2013**, *4*, 1894−1900.
(141) Rakhi, R.; Alhebshi, N.-A.; Anjum, D.-H.; Alshareef, H.-N. Nanostructured Cobalt Sulfide-on-Fiber with Tunable Morphology as Electrodes for Asymmetric Hybrid Supercapacitors. *J. Mater. Chem. A* **2014**, *2*, 16190−16198.
(142) Hu, H.; Guan, B. Y.; Lou, X.-W.-D. Construction of Complex CoS Hollow Structures with Enhanced Electrochemical Properties for Hybrid Supercapacitors. *Chem.* **2016**, *1*, 102−113.
(143) Jiang, Z.; Lu, W.; Li, Z.; Ho, K.-H.; Li, X.; Jiao, X.; Chen, D. Synthesis of Amorphous Cobalt Sulfide Polyhedral Nanocages for High Performance Supercapacitors. *J. Mater. Chem. A* **2014**, *2*, 8603−8606.
(144) Salunkhe, R.-R.; Tang, J.; Kamachi, Y.; Nakato, T.; Kim, J.-H.; Yamauchi, Y. Asymmetric Supercapacitors Using 3D Nanoporous Carbon and Cobalt Oxide Electrodes Synthesized from a Single Metal-Organic Framework. *ACS Nano* **2015**, *9*, 6288−6296.
(145) Chen, W.; Xia, C.; Alshareef, H.-N. One-Step Electrodeposited Nickel Cobalt Sulfide Nanosheet Arrays for High-Performance Asymmetric Supercapacitors. *ACS Nano* **2014**, *8*, 9531−9541.
(146) Yu, D.; Wu, B.; Ge, L.; Wu, L.; Wang, H.; Xu, T. Decorating Nanoporous ZIF-67-Derived $NiCo_2O_4$ Shells on a Co_3O_4 Nanowire Array Core for Battery-Type Electrodes with Enhanced Energy Storage Performance. *J. Mater. Chem. A* **2016**, *4*, 10878−10884.
(147) Cheong, J. Y.; Koo, W. T.; Kim, C.; Jung, J.-W.; Kim, I.-D. Feasible Defect Engineering by Employing Metal Organic Framework Templates into One-Dimensional Metal Oxides for Battery Applications. *ACS Appl. Mater. Interfaces* **2018**, *10*, 20540−20549.
(148) Tian, W.; Hu, H.; Wang, Y.; Li, P.; Liu, J.; Liu, J.; Wang, X.; Xu, X.; Li, Z.; Zhao, Q.; Ning, H.; Wu, W.; Wu, M. Metal-Organic Frameworks Mediated Synthesis of One-Dimensional Molybdenum-Based/Carbon Composites for Enhanced Lithium Storage. *ACS Nano* **2018**, *12*, 1990−2000.
(149) Zhang, C.; Tian, J.; Rao, W.; Guo, B.; Fan, L.; Xu, W.; Xu, J. Polypyrrole@Metal-Organic Framework (UIO-66)@Cotton Fabric Electrodes for Flexible Supercapacitors. *Cellulose* **2019**, *26*, 3387−3399.
(150) Guo, S. N.; Zhu, Y.; Yan, Y. Y.; Min, Y. L.; Fan, J. C.; Xu, Q. J.; Yun, H. (Metal-Organic Framework)-Polyaniline Sandwich Structure Composites as Novel Hybrid Electrode Materials for High-Performance Supercapacitor. *J. Power Sources* **2016**, *316*, 176−182.
(151) Liu, Y.; Xu, N.; Chen, W.; Wang, X.; Sun, C.; Su, Z. Supercapacitor with High Cycling Stability Through Electrochemical Deposition of Metal-Organic Frameworks/Polypyrrole Positive Electrode. *Dalton T.* **2018**, *47*, 13472−13478.
(152) Ehsani, A.; Khodayari, J.; Hadi, M.; Shiri, H. M.; Mostaanzadeh, H. Nanocomposite of p-Type Conductive Polymer/Cu (II)-Based Metal-Organic Frameworks as A Novel and Hybrid Electrode Material for Highly Capacitive Pseudocapacitors. *Ionics* **2017**, *23*, 131−138.
(153) Zhu, X.; Li, J.; Ali, R. N.; Huang, M.; Liu, P.; Xiang, B. Toward a High-Performance Li-Ion Battery: Constructing a $Co_{1-x}S$/ZnS@C Composite Derived from Metal-Organic Framework@3D Disordered Polystyrene Sphere Template. *Mater. Des.* **2018**, *160*, 636−641.
(154) Zhou, S.; Kong, X.; Zheng, B.; Huo, F.; Strømme, M.; Xu, C. Cellulose Nanofiber@Conductive Metal-Organic Frameworks for High-Performance Flexible Supercapacitors. *ACS Nano* **2019**, *13*, 9578−9586.
(155) Salunkhe, R. R.; Tang, J.; Kobayashi, N.; Kim, J.; Ide, Y.; Tominaka, S.; Kim, J. H.; Yamauchi, Y. Ultrahigh Performance Supercapacitors Utilizing Core-Shell Nanoarchitectures from A Metal-Organic Framework-Derived Nanoporous Carbon and A Conducting Polymer. *Chem. Sci.* **2016**, *7*, 5704−5713.
(156) Wang, H. N.; Zhang, M.; Zhang, A. M.; Shen, F.-C.; Wang, X.-K.; Sun, S.-N.; Chen, Y.-J.; Lan, Y.-Q. Polyoxometalate-Based Metal-Organic Frameworks with Conductive Polypyrrole for Supercapacitors. *ACS Appl. Mater. Interfaces* **2018**, *10*, 32265−32270.
(157) Xu, X.; Tang, J.; Qian, H.; Hou, S.; Bando, Y.; Hossain, M. S. A.; Pan, L.; Yamauchi, Y. Three-Dimensional Networked Metal-Organic Frameworks with Conductive Polypyrrole Tubes for Flexible Supercapacitors. *ACS Appl. Mater. Interfaces* **2017**, *9*, 38737−38744.
(158) Sheberla, D.; Bachman, J. C.; Elias, J. S.; Sun, C.-J.; Shao-Horn, Y.; Dincă, M. Conductive MOF Electrodes for Stable Supercapacitors with High Areal Capacitance. *Nat. Mater.* **2017**, *16*, 220−224.
(159) Feng, D.; Lei, T.; Lukatskaya, M. R.; Park, J.; Huang, Z.; Lee, M.; Shaw, L.; Chen, S.; Yakovenko, A. A.; Kulkarni, A.; Xiao, J.; Fredrickson, K.; Tok, J. B.; Zou, X.; Cui, Y.; Bao, Z. Robust and conductive two-dimensional metal−organic frameworks with exceptionally high volumetric and areal capacitance. *Nat. Energy* **2018**, *3*, 30−36.
(160) Li, W.-H.; Ding, K.; Tian, H.-R.; Yao, M.-S.; Nath, B.; Deng, W.-H.; Wang, Y.; Xu, G. Conductive metal-organic framework nanowire array electrodes for high-performance solid-state supercapacitors. *Adv. Funct. Mater.* **2017**, *27*, 1702067.

https://dx.doi.org/10.1021/acsanm.0c00702
ACS Appl. Nano Mater. 2020, 3, 3964−3990